Journal of Neuroinflammation

RESEARCH

Open Access

# A transient blood IL-17 increase triggers neuroinflammation in cerebellum and motor incoordination in hyperammonemic rats

Yaiza M. Arenas[1,2,3], Carmina Montoliu[2,3], Marta Llansola[1] and Vicente Felipo[1*]

## Abstract

Patients with liver cirrhosis may show minimal hepatic encephalopathy (MHE) with motor incoordination which is reproduced in hyperammonemic rats. Hyperammonemia induces peripheral inflammation which triggers neuroinflammation and enhanced GABAergic neurotransmission in cerebellum and motor incoordination. The mechanisms involved remain unknown. The aims were to assess if the early increase of peripheral IL-17 triggers motor incoordination in hyperammonemic rats and to identify some underlying mechanisms. We assessed if blocking peripheral IL-17 with anti-IL-17 at 2–4 days of hyperammonemia prevents motor incoordination and analyzed underlying mechanisms. Hyperammonemia induces a transient blood IL-17 increase at days 3–4. This is associated with increased IL-17 receptor membrane expression and activation in cerebellum, leading to NADPH oxidase activation, increased superoxide production and MLCK that induce blood–brain barrier (BBB) permeabilization by reducing occludin and ZO-1. BBB permeabilization facilitates the entry of IL-17, which increases in cerebellum and activates microglia. This increases TNFα and the TNFR1-S1PR2-CCL2-BDNF-TrkB pathway. This enhances GABAergic neurotransmission which impairs motor coordination. Blocking peripheral IL-17 with anti-IL-17 prevents all the above process and prevents motor incoordination. Early treatment to reduce blood IL-17 may be a useful treatment to reverse motor incoordination in patients with MHE.

**Keywords** Hyperammonemia, Hepatic encephalopathy, Motor incoordination, IL-17, Blood–brain barrier, Neuroinflammation, GABAergic neurotransmission, Anti-IL-17, Therapeutic treatment

*Correspondence:
Vicente Felipo
vfelipo@cipf.es
Full list of author information is available at the end of the article

**Graphical abstract**

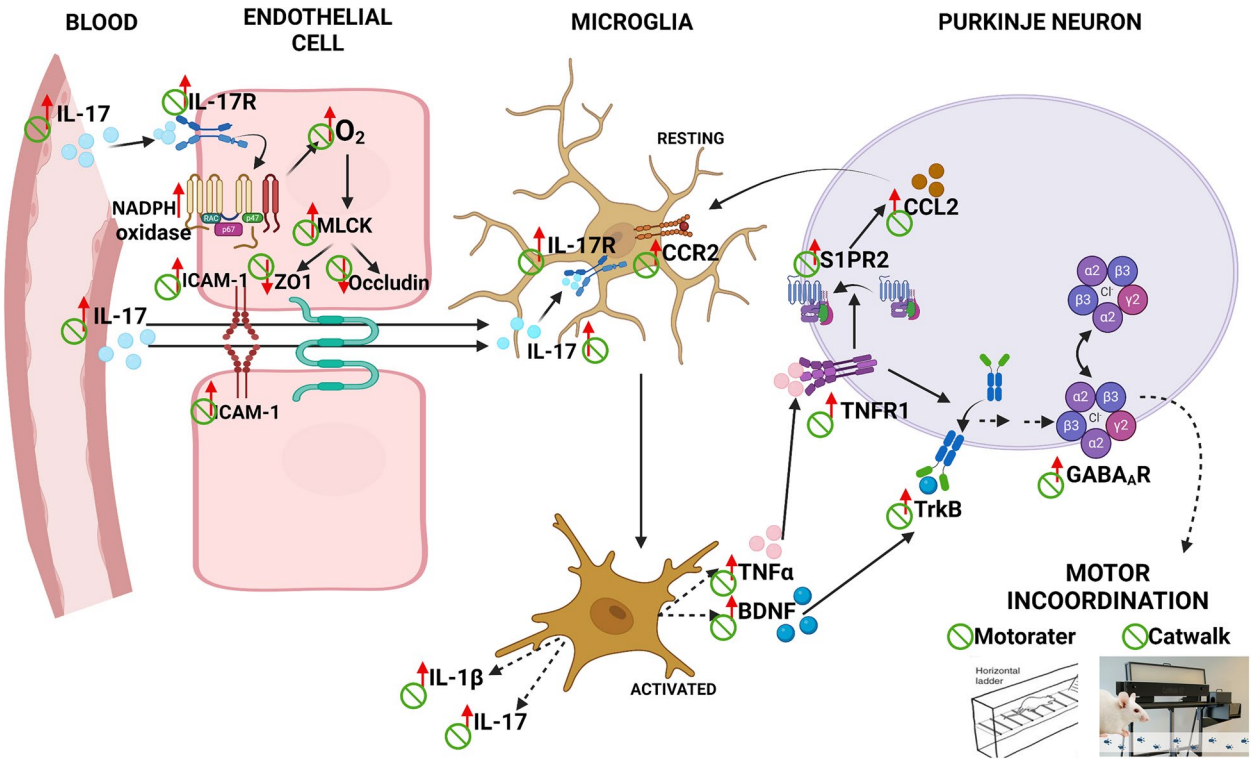


## Introduction

Patients with liver cirrhosis may show minimal hepatic encephalopathy (MHE) with mild cognitive impairment, psychomotor slowing and motor incoordination which reduce their quality of life and life span. Hyperammonemia and inflammation act synergistically to induce MHE [1–6]. Rats with chronic hyperammonemia reproduce most of the cognitive and motor alterations present in patients with MHE and have been used to investigate the mechanisms leading to MHE. Hyperammonemia induces peripheral inflammation which triggers neuroinflammation in cerebellum and hippocampus. Neuroinflammation in turn alters GABAergic and glutamatergic neurotransmission leading to motor incoordination and cognitive impairment [7–11].

Motor incoordination in rats with hyperammonemia and MHE is a consequence of enhanced GABAergic neurotransmission in cerebellum due to increased levels of GABA, increased membrane expression of $GABA_A$ receptors and of the chloride co-transporter KCC2 [9, 10]. These changes in turn are a consequence of neuroinflammation. Increased levels of TNFα and of membrane expression of its receptor TNFR1 enhance the activation of the TNFR1-S1PR2-CCR2-BDNF-TrkB pathway and of microglia in cerebellum which induce the enhancement of GABAergic neurotransmission [9, 10].

Hyperammonemic rats show neuroinflammation, with activation of microglia and astrocytes and increased levels of TNFα in cerebellum and hippocampus. The induction of neuroinflammation by hyperammonemia is mediated by peripheral inflammation and is prevented if hyperammonemia-induced peripheral inflammation is prevented with anti-TNFα [7]. Peripheral inflammation also induces neuroinflammation in other pathological situations, including Parkinson's and Alzheimer's disease and multiple sclerosis [12–17] and has been proposed as a common link to progressive neurological diseases [18].

However, the mechanisms by which hyperammonemia-induced peripheral inflammation triggers neuroinflammation are not well known.

In cirrhotic patients appearance of MHE is triggered by a shift in the immunophenotype and peripheral inflammation to an "autoimmune-like" form with enhanced activation of CD4 lymphocytes, especially of

Th17, which produces IL-17, and increased blood levels of IL-17 and other pro-inflammatory cytokines which promote the infiltration of lymphocytes and monocytes into the brain [19, 20]. Moreover, patients died with liver cirrhosis or steatohepatitis show infiltration of CD4 lymphocytes, especially of Th17, into the meninges of cerebellum and hippocampus [21, 22]. Infiltration of monocytes into the brain has been also reported in other animal models of MHE [23, 24]. This suggests that increased peripheral IL-17 could play a role in triggering MHE in cirrhotic patients. IL-17 also plays a key role in triggering multiple sclerosis pathology [25, 26] and in other neurological diseases such as autism spectrum disorder, Alzheimer's disease, epilepsy, and depression [27].

It has been reported that IL-17 induces permeabilization of the blood brain barrier (BBB) and may cross it [28–30]. IL-17 receptors are expressed by the endothelial cells on the blood–brain barrier in multiple sclerosis lesions. Peripheral IL-17 disrupts BBB tight junctions in vitro and in vivo, promoting BBB disruption and neuroinflammation [28]. IL-17 also increases BBB permeability in an in vitro model and this was associated with reduced content of occluding and ZO-1 [29].

Huppert et al. [31], showed that a main mechanism by which peripheral IL-17 may induce permeabilization of the BBB is by activating the IL-17 receptor in endothelial cells, which increases NADPH oxidase activity by increasing membrane expression of phox67 and phox47, leading to increased formation of superoxide which increases MLCK, leading to reduced occludin and ZO-1 [31–34].

Rodrigo et al. [35] and Balzano et al. [36], showed that microglia are activated in cerebellum of hyperammonemic rats already at seven days of hyperammonemia.

We found that hyperammonemia induces a transient increase in peripheral blood IL-17 levels at 3–4 days of hyperammonemia, just before appearance of neuroinflammation in brain. We hypothesized that the increased levels of IL-17 in blood could trigger neuroinflammation, alterations in neurotransmission and motor incoordination in hyperammonemic rats and that this could be mediated by permeabilization of the BBB.

The aims of this work were to assess if the early increase of peripheral IL-17 at 3–4 days of hyperammonemia triggers motor incoordination in hyperammonemic rats and to identify some of the underlying mechanisms. We assessed if blocking peripheral IL-17 with anti-IL-17 at 2–4 days of hyperammonemia affords a sustained prevention of the induction of motor incoordination in hyperammonemic rats. We also analyzed if prevention of motor incoordination is associated with prevention of the enhancement in cerebellum of neuroinflammation and of GABAergic neurotransmission. We also assessed if at 4 days of hyperammonemia rats show BBB permeabilization and if this is prevented by blocking peripheral IL-17 with anti-IL17. The experimental design is summarized in Fig. 1.

## Results

### Rats show a peak of IL-17 in blood at 3–4 days of hyperammonemia

We analyzed the time-course of the changes of IL-17 in blood induced by eating the ammonia-containing diet. This diet induced a sustained increase of ammonia levels in blood (Fig. 2A). Hyperammonemia induced a transient increase in the plasma levels of IL-17 (Fig. 2B) which was significantly increased at 3 days of hyperammonemia but decreased to normal levels, not different from control rats at 7 days of hyperammonemia. At 4 weeks of hyperammonemia plasma levels of IL-17 were similar to control rats (Fig. 2B).

### Early transient blockade of blood IL-17 affords sustained prevention of motor impairment in hyperammonemic rats

To assess the effects of blocking peripheral IL-17 on motor function, rats were injected with anti-IL-17 on days 2, 3 and 4 after beginning the ammonia-containing diet. Motor coordination was analyzed at 2 weeks of hyperammonemia in the motorater. Hyperammonemic rats show motor incoordination as indicated by the increased number of wrong foot placements (Fig. 3A) and of total errors per run (Fig. 3B). The induction of motor incoordination at 2 weeks of hyperammonemia was prevented by the early injection of anti-IL17. Hyperammonemic rats injected with anti-IL-17 did not show increased number of wrong foot placements (Fig. 3A) or of total errors per run (Fig. 3B).

Motor coordination was also analyzed at 2 weeks of hyperammonemia in the Catwalk by measuring the regularity index, which was reduced in hyperammonemic rats, indicating motor incoordination, but not in hyperammonemic rats injected with anti-IL-17 at 2–4 days of hyperammonemia (Fig. 3C). Hyperammonemia also increased the initial dual stance in the Catwalk, which was also prevented by early anti-IL-17 injection (Fig. 3D).

The prevention of impairment of motor function by early injection of anti-IL-17 is not due to reduction of hyperammonemia. Blood ammonia levels were not reduced by anti-IL-17 injection at 4 weeks of ingestion of the ammonia-containing diet (Fig. 3E).

### Early transient blockade of blood IL-17 prevents enhancement of GABAergic neurotransmission in cerebellum of hyperammonemic rats

We have previously shown that motor incoordination in hyperammonemic rats is due to enhanced GABAergic neurotransmission in cerebellum [9, 10, 37, 38].

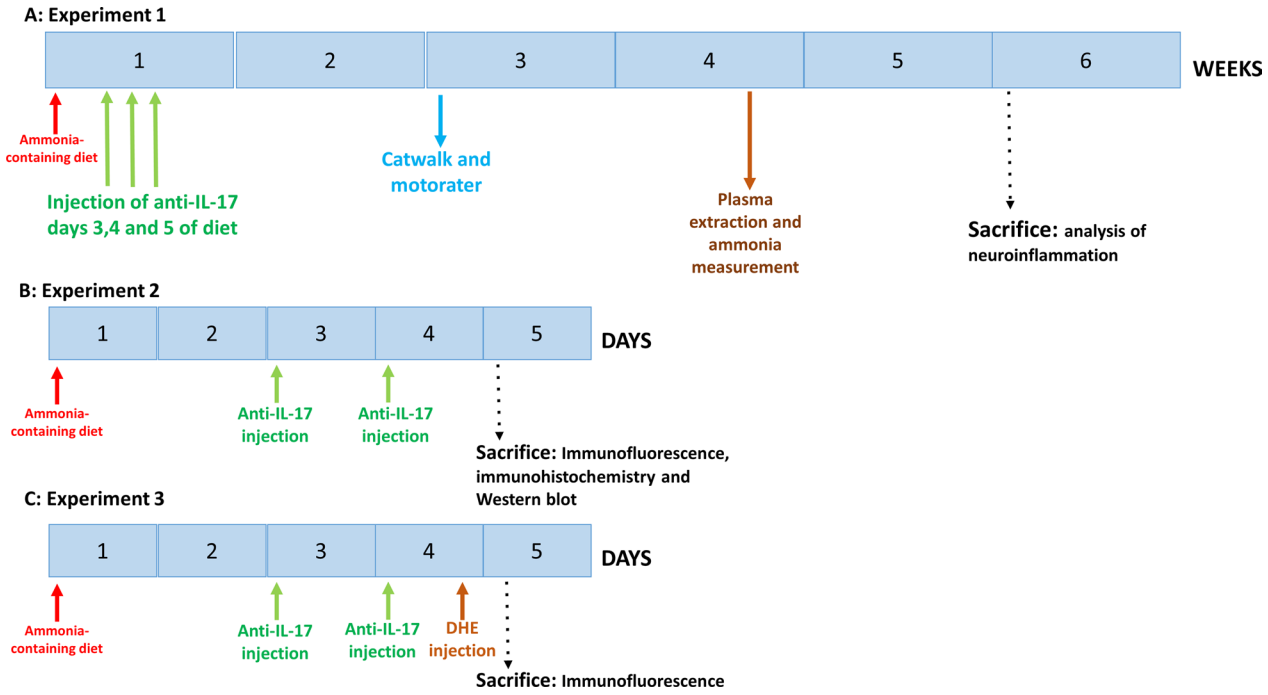


**Fig. 1** Experimental design. **A** Experiment 1: To assess if transient blocking of peripheral IL-17 affords sustained prevention of motor impairment. Rats were injected in the tail vein with anti-IL-17 or vehicle after 2, 3 and 4 days of hyperammonemia. Motor coordination was analyzed after 2 weeks of hyperammonemia. Rats were sacrificed after 5 weeks of hyperammonemia. **B** Experiment 2. To analyze underlying mechanisms, rats were injected in the tail vein with anti-IL-17 or vehicle after 2 and 3 days of hyperammonemia and sacrificed at 4th days. Some rats were perfused for immunohistochemistry and immunofluorescence analysis and others for Western blot analysis of protein content and membrane expression. **C** Experiment 3: To analyze the production of superoxide in endothelial cells in cerebellum, rats were injected with anti-IL-17 as in experiment 2, but, in addition, after 3 days of hyperammonemia rats were also injected i.p. with dihydroethidium (DHE). After 18 h of DHE injection rats were perfused for immunofluorescence analysis

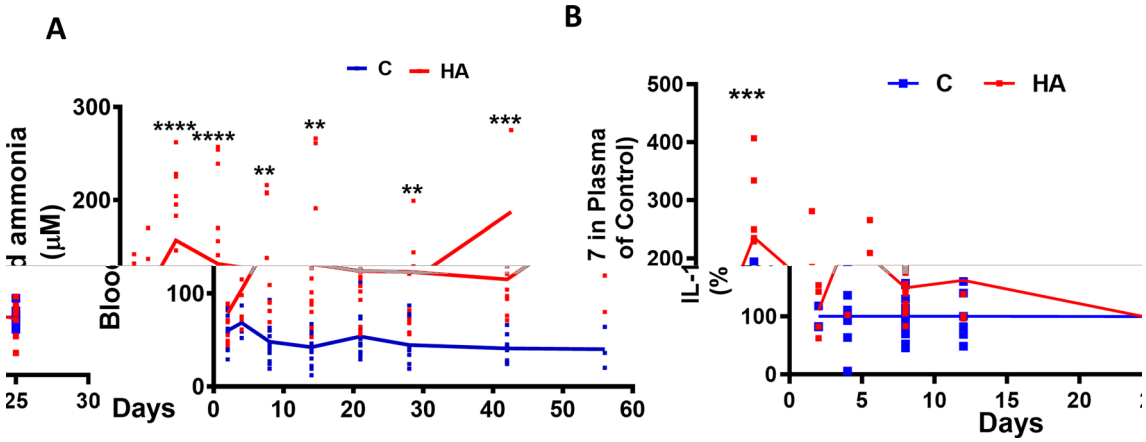


**Fig. 2** Hyperammonemic rats show a sustained increase of blood ammonia and a transient increase in plasma IL-17. Blood ammonia (**A**) and plasma IL-17 (B) were measured as described in methods. Blood amoonia (**A**) was measured at 2, 4, 8, 14, 21, 28, 42 and 56 days of hyperammonemia and IL-17 (**B**) was measured at 2, 4, 8, 12 and 25 days of hyperammonemia. Values are the mean ± SEM of 3–16 rats/group for ammonia and 4–14 rats/group for IL-17. Values significantly different from control rats using two-way ANOVA (NewmanKeuls multiple post-hoc) are indicated by asterisks (**p < 0.01, ***p < 0.001, ****p < 0.0001)

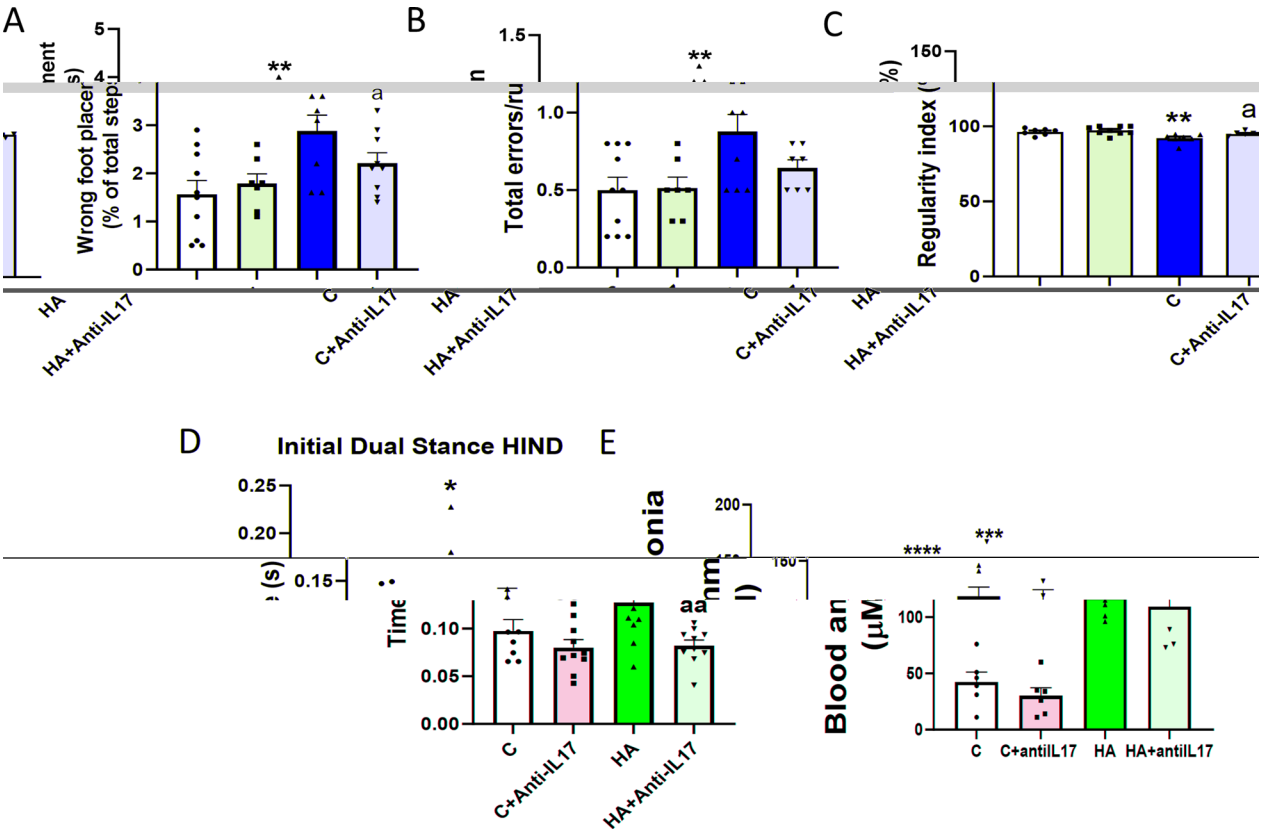


**Fig. 3** Anti-IL-17 prevents motor incoordination but not the increase in blood ammonia in hyperammonemic rats. Motor coordination was assessed in the Motorater by analyzing wrong foot placements (slips) (**A**) and the total errors per run (**B**) and in the Catwalk™: **C**: Regularity index. The initial dual stance hind (**D**) was also analyzed in the Catwalk.™. Blood ammonia (**E**) was measured at 4 weeks of hyperammonemia as described in methods. Values are the mean ± SEM of 10 rats/group in **A**–**J** and n = 6 rats/group in **K**. One-way ANOVA followed by Fisher's LSD post-hoc test was performed to compare all groups. Values significantly different from control group are indicated by asterisk. (*p < 0.05, **p < 0.01, ***p < 0.001, ****p < 0.0001) and values significantly different from HA group are indicated by a (a = p < 0.05, aa = p < 0.01). C = control rats injected with vehicle; C + Anti-IL-17: control rats injected with anti-IL-17; HA: hyperammonemic rats injected with vehicle; HA + Anti-IL-17: hyperammonemic rats injected with anti-IL-17

We assessed if anti-IL-17 would prevent the impairment of motor incoordination by preventing enhancement of GABAergic neurotransmission. Two main changes contributing to enhanced GABAergic neurotransmission at 4–5 weeks of hyperammonemia are the increased membrane expression of several $GABA_A$ receptor subunits and of the chloride co-transporters KCC2 and NKCC1 [9, 10]. We analyzed in cerebellum of rats at 4 days of hyperammonemia the effects of hyperammonemia and of injection of anti-IL-17 on these main parameters involved in the enhancement of GABAergic neurotransmission.

The membrane expression of the α2 (Fig. 4A), β3 (Fig. 4B) and γ2 (Fig. 4C) subunits of $GABA_A$ receptors was also increased in cerebellum of hyperammonemic rats at 4 days of hyperammonemia. The increase in membrane expression of all these subunits was prevented by early injection of anti-IL-17 (Fig. 4A–C).

Hyperammonemia also increases the membrane expression of KCC2 (Fig. 4D) and NKCC1 (Fig. 4E) in cerebellum at 4 days of hyperammonemia and these increases were also prevented by early injection of anti-IL-17.

These results show that enhancement of GABAergic neurotransmission is already present in cerebellum at 4 days of hyperammonemia and it is prevented by early injection of anti-IL-17.

### Early transient blockade of blood IL-17 prevents enhancement of the TNFα-TNFR1-S1PR2-CCL2-CCR2-BDNF-TrkB pathway in cerebellum of hyperammonemic rats

We have previously shown that enhanced GABAergic neurotransmission in cerebellum at 4–5 weeks of hyperammonemia is a consequence of enhanced activation of the TNFα-TNFR1-S1PR2-CCL2-CCR2-BDNF-TrkB pathway and of microglia [9, 10]. We assessed if

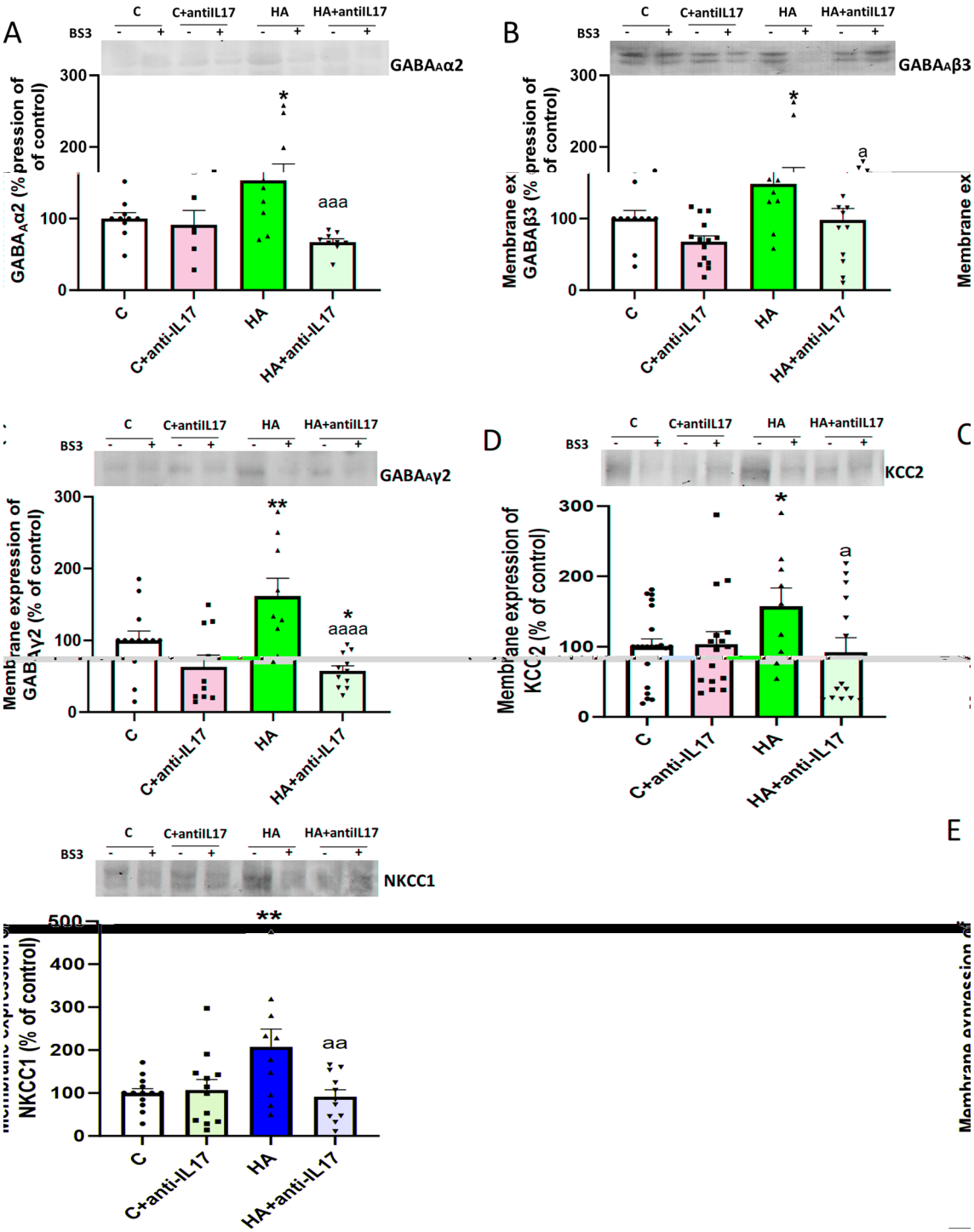


**Fig. 4** Injection with anti-IL-17 prevents the alterations in the GABAergic neurotransmission in cerebellum of hyperammonemic rats at 4 days of hyperammonemia. Membrane expression of (**A**) $GABA_A\alpha2$, (**B**) $GABA_A\beta3$, (**C**) $GABA_A\gamma2$, (**D**) KCC2, and (**E**) NKCC1 were analyzed using BS3 cross-linker. Representative images of the blots for each protein are shown. Values are expressed as percentage of controls and are the mean ± SEM of 7 rats/group. One-way ANOVA followed by Fisher's LSD post-hoc test was performed to compare all groups. Values significantly different from controls are indicated by asterisk (*$p < 0.05$, **$p < 0.01$) and values significantly different from HA group are indicated by a ($a = p < 0.05$, $aa = p < 0.01$, $aaa = p < 0.001$, $aaaa = p < 0.0001$)

anti-IL-17 would prevent the enhancement of GABAergic neurotransmission by preventing the increased function of the TNFα-TNFR1-S1PR2-CCL2-CCR2-BDNF-TrkB pathway and microglia activation.

At 4 days of hyperammonemia the membrane expression of TNFR1 (Fig. 5A) and of S1PR2 (Fig. 5B) are increased in cerebellum of hyperammonemic rats. The increase in membrane expression of these receptors was prevented by early injection of anti-IL-17 (Fig. 5A, B). Hyperammonemia also increases the content of CCL2 (Fig. 5C), membrane expression of CCR2 (Fig. 5D), the content of BDNF (Fig. 5E) and TrkB (Fig. 5F) and membrane expression of TrkB (Fig. 5G) at 4 days. This reproduces the increased activation of the TNFα-TNFR1-S1PR2-CCL2-CCR2-BDNF-TrkB pathway reported at 4–5 weeks of hyperammonemia [9, 10]. All these changes at 4 days are also prevented by early injection of anti-IL-17 (Fig. 5A–G).

#### Early transient blockade of blood IL-17 prevents microglia activation and the increase in pro-inflammatory factors in cerebellum of hyperammonemic rats

Activation of the TNFα-TNFR1-S1PR2-CCL2-CCR2-BDNF-TrkB pathway is associated with microglia activation in cerebellum at 4–5 weeks of hyperammonemia [9, 10].

At 4 days of hyperammonemia, microglia is already activated in white matter of the cerebellum, as indicated by the reduced area (Fig. 6A, C), perimeter (Fig. 6A, D) and roundness (Fig. 6A, E). At this time of hyperammonemia we did not observe any activation of astrocytes (Fig. 6B, F). Injection of anti-IL-17 prevented the activation of microglia in hyperammonemic rats. The area (Fig. 6A, C), perimeter (Fig. 6A, D) and roundness (Fig. 6A, E) of microglia in hyperammonemic rats injected with anti-IL-17 were similar to those of control rats. Anti-IL-17 slightly reduced astrocyte activation in hyperammonemic rats (Fig. 6B, F).

Microglia activation was associated with increased levels of pro-inflammatory cytokines. At 4 days of hyperammonemia rats show increased levels of pro-inflammatory TNFα (Fig. 6G) and IL-1β (Fig. 6H) and reduced content of the anti-inflammatory IL-10 (Fig. 6I) in cerebellum. All these changes were also prevented by early injection of anti-IL17 (Fig. 6G–I).

#### Early transient blockade of blood IL-17 prevents the increase in IL-17 receptor activation and blood–brain barrier (BBB) permeabilization in cerebellum of hyperammonemic rats

The content of IL-17 (Fig. 7A) and the membrane expression of the IL-17 receptor (Fig. 7B) were increased in cerebellum at 4 days of hyperammonemia. These changes were prevented by early injection of IL-17 (Fig. 7A,B). The content of the tight junction proteins occludin (Fig. 7C) and ZO-1 (Fig. 7D) as well as claudin 10 (Fig. 7E) were reduced in cerebellum at 4 days of hyperammonemia and this reduction was prevented by injection of anti-IL-17 (Fig. 7C–E).

To assess if the reduction of occludin and ZO-1 content could be mediated by enhanced activation of NADPH oxidase, we analyzed the membrane surface expression of phox67 and phox47. Both phox67 (Fig. 7F) and phox47 (Fig. 7G) are increased in the membrane surface in cerebellum of hyperammonemic rats at 4 days of hyperammonemia, indicating activation of NADPH oxidase and this increase is prevented by early injection of anti-IL-17 (Fig. 7F,G).

Activation of NADPH oxidase is associated with increased superoxide production in endothelial cells, as shown in Fig. 8. Endothelial cells were labeled with CD31 and the production of superoxide in CD31 positive cells in cerebellar meninges was analyzed with DHE as described in methods. Hyperammonemia increases the formation of superoxide in endothelial cells (Fig. 8A, B) and this is prevented by early injection of anti-IL-17.

The increased formation of superoxide is associated with increased levels of MLCK (Fig. 8C), which would induce the loss of occluding and ZO-1, resulting in BBB permeabilization [31–34].

#### Early transient blockade of blood IL-17 prevents the infiltration of Th17 CD4 lymphocytes and of macrophages in cerebellar meninges of hyperammonemic rats

At 4 days of hyperammonemia rats show infiltration in cerebellar meninges CD4 lymphocytes (Fig. 9A, D). Double immunofluorescence staining with CD4 and IL-17 shows that there is an infiltration of Th17 CD4 lymphocytes in the cerebellar meninges of hyperammonemia rats (Fig. 9B, E). Moreover, there is also infiltration of macrophages (stained with Iba1) (Fig. 9C, F). The infiltration of total CD4 lymphocytes, Th17 CD4 lymphocytes and monocytes was prevented by injection of anti-IL-17 (Fig. 9). The contents in cerebellar homogenates of CD4 (Fig. 9G) and of ICAM1 (Fig. 9H), which facilitates immune cells infiltration, are also increased in hyperammonemic rats and these increases are also prevented by anti-IL-17 (Fig. 9G, H).

#### Early transient blockade of blood IL-17 affords sustained prevention of the enhancement of GABAergic neurotransmission and BBB permeabilization in cerebellum of hyperammonemic rats

To find out if the effects induced after 4 days of hyperammonemia by the transient blockade of blood IL-17

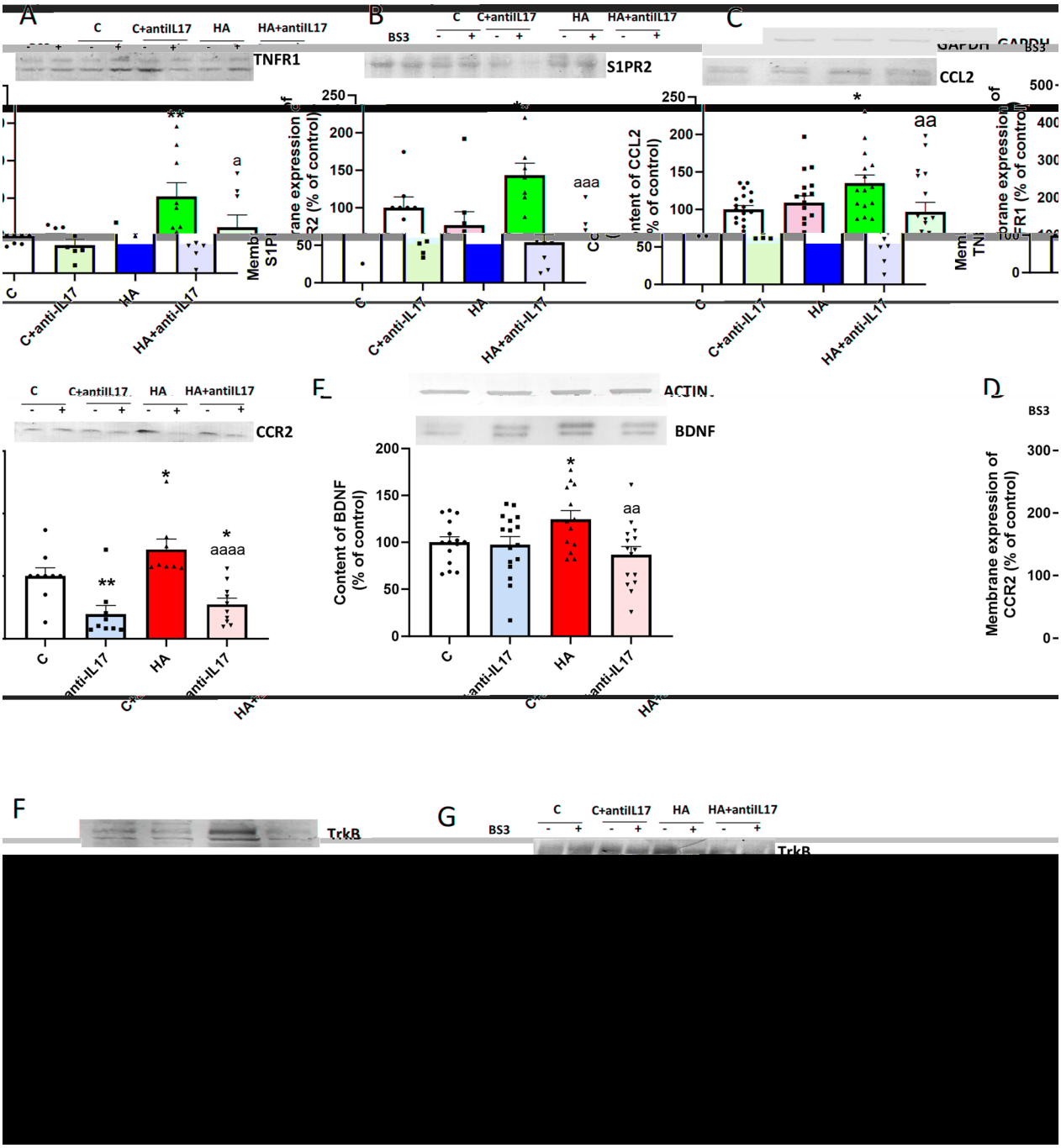


**Fig. 5** Injection with anti-IL-17 prevents the alterations in the TNFα-TNFR1- S1PR2-CCL2-BDNF-TrkB pathway in cerebellum of hyperammonemic rats. Membrane expression of (**A**) TNFR1, (**B**) S1PR2, (**D**) CCR2 and (**G**) TrKB were analyzed using BS3 cross-linker. Protein content of (**C**) CCL2, (**E**) BDNF and (**F**) TrKB in cerebellum, was analyzed by Western blot. Representative images of the blots of each protein are shown. Values are expressed as percentage of controls and are the mean ± SEM of 7 rats/group. One-way ANOVA followed by Fisher's LSD post-hoc test was performed to compare all groups. Values significantly different from controls are indicated by asterisk (*$p < 0.05$, **$p < 0.01$) and values significantly different from HA group are indicated by a (a = $p < 0.05$, aa = $p < 0.01$, aaa = $p < 0.001$, aaaa = $p < 0.0001$)

are maintained over time or are also transient, we evaluated the effects of blocking IL-17 by injecting anti-IL-17 at days 2–4 of hyperammonemia on GABAergic neurotransmission and BBB permeability at 5 weeks of hyperammonemia.

The effects on GABAergic neurotransmission were evaluated as in point 2.3. The membrane expression of the α2 (Fig. 10A), β3 (Fig. 10B) and γ2 (Fig. 10C) subunits of $GABA_A$ receptors were also increased in cerebellum of hyperammonemic rats at 5 weeks of hyperammonemia. The increase in membrane expression of all these subunits was prevented by early injection of anti-IL-17 (Fig. 10A–C).

Hyperammonemia also increases the membrane expression of KCC2 (Fig. 10D) and NKCC1 (Fig. 10E) in cerebellum at 5 weeks of hyperammonemia and these increases were also prevented by early injection of anti-IL-17.

These results show that early transient blockade of blood IL-17 affords sustained prevention of the enhancement of GABAergic neurotransmission for at least 5 weeks.

We also analyzed the effects on BBB permeability as in point 2.6. The content of occludin (Fig. 11A), of ZO-1 (Fig. 11B) and of claudin 10 (Fig. 11C) were also reduced in cerebellum at 5 weeks of hyperammonemia and this reduction was prevented by injection of anti-IL-17 (Fig. 11A–C).

To assess if the reduction of occludin and ZO-1 content could be mediated by enhanced activation of NADPH oxidase, we analyzed the membrane surface expression of phox67 and phox47. Both phox67 (Fig. 11D) and phox47 (Fig. 11E) are increased in the membrane surface in cerebellum of hyperammonemic rats at 5 weeks of hyperammonemia, indicating activation of NADPH oxidase and this increase is prevented by early injection of anti-IL-17 (Fig. 11D, E). These results show that early transient blockade of blood IL-17 also affords sustained prevention of the permeabilization of the BBB for at least 5 weeks.

### Early transient blockade of blood IL-17 reduces pro-inflammatory cytokines in plasma of hyperammonemic rats

We have previously shown that systemic inflammation is a crucial intermediary between hyperammonemia, neuroinflammation and neurological impairment [7, 8]. We therefore assessed if anti-IL-17 treatment reduces pro-inflammatory cytokines in plasma of hyperammonemic rats. As shown in Table 1, at 3 days of hyperammonemia, plasma levels of pro-inflammatory TNFα, IL-17, IL-18, IL-22, CCL2 and CCL5 are increased. TNF-α, IL-17, IL-18, IL-22, CCL2, CCL5 and increases TGFβ, IL-4 and IL-10. Treatment with anti-IL-17 reduces plasma levels of TNF-α, IL-17, IL-18, IL-22, CCL2, CCL5 and increases the anti-inflammatory cytokines TGFβ, IL-4 and IL-10.

## Discussion

The results reported are summarized in Fig. 12. Hyperammonemia induces an early transient increase of IL-17 in blood during days 2–4 of hyperammonemia. IL-17 activates the IL-17 receptor leading to translocation to the membrane surface of phox67 and phox47 subunits of NADPH oxidase leading to its activation and increased formation of superoxide in endothelial cells. This increases MLCK leading to reduced content of occluding and ZO-1 and to permeabilization of the BBB. Moreover, the levels of ICAM-1 are increased. This, together with the BBB permeabilization triggers the infiltration of IL-17 and the increase of IL-17 levels in cerebellum. Enhanced activation of the IL-17 receptor triggers microglia activation, leading to increased production of pro-inflammatory cytokines (TNFα, IL-1β, IL-17) and of BDNF and to increased membrane expression of TNFR1, S1PR2, CCR2 and TrkB. The enhanced activation of the TNFα-TNFR1-S1PR2-CCL2-CCR2-BDNF-TrkB pathway leads to increased membrane expression of $GABA_A$ receptor subunits and of KCC2, resulting in enhanced GABAergic neurotransmission in cerebellum. This leads to motor incoordination. Hyperammonemia also induces cognitive impairment by enhancing neuroinflammation and altering neurotransmission in hippocampus [7, 39].

These results show that 4 days of hyperammonemia are enough to induce most changes observed in cerebellum at 4–5 weeks of hyperammonemia: CD4 lymphocytes infiltration, microglia activation, enhanced function of the TNFα-TNFR1-S1PR2-CCL2-CCR2-BDNF-TrkB pathway and of GABAergic neurotransmission [9, 10]. However, hyperammonemia at 4 days does not induce astrocyte activation, which is observed in cerebellum at 4–5 weeks of hyperammonemia. It has been proposed that activated microglia and infiltrating

(See figure on next page.)

**Fig. 6** Early injection of anti-IL-17 prevents microglia activation and the increase in pro-inflammatory factors in cerebellum of hyperammonemic rats. Representative images of immunohistochemistry against Iba1 in white matter (**A**) and GFAP (**B**). The area (**C**), perimeter (**D**) and roundness (**E**) of microglia (Iba1 stained cells) in white matter are expressed in $\mu m^2$, μm and arbitrary units, respectively. The reduced area, perimeter and roundness reflects prevention of morphological activation of microglia by anti-IL-17 injection. GFAP stained area expressed as percentage of total area (**F**). Protein content of (**G**) TNFα, (**H**) IL1β and (**I**) IL-10 was analyzed by Western blot. One-way ANOVA followed by Fisher's LSD post-hoc test was performed to compare all groups. Values are the mean ± SEM of 3 rats/group in **A**–**F** and 7 rats/group in (G-I). Values significantly different from control group are indicated by asterisk (*$p < 0.05$, **$p < 0.01$) and values significantly different from HA group are indicated by a (a = $p < 0.05$, aa = $p < 0.01$, aaa = $p < 0.001$, aaaa = $p < 0.0001$)

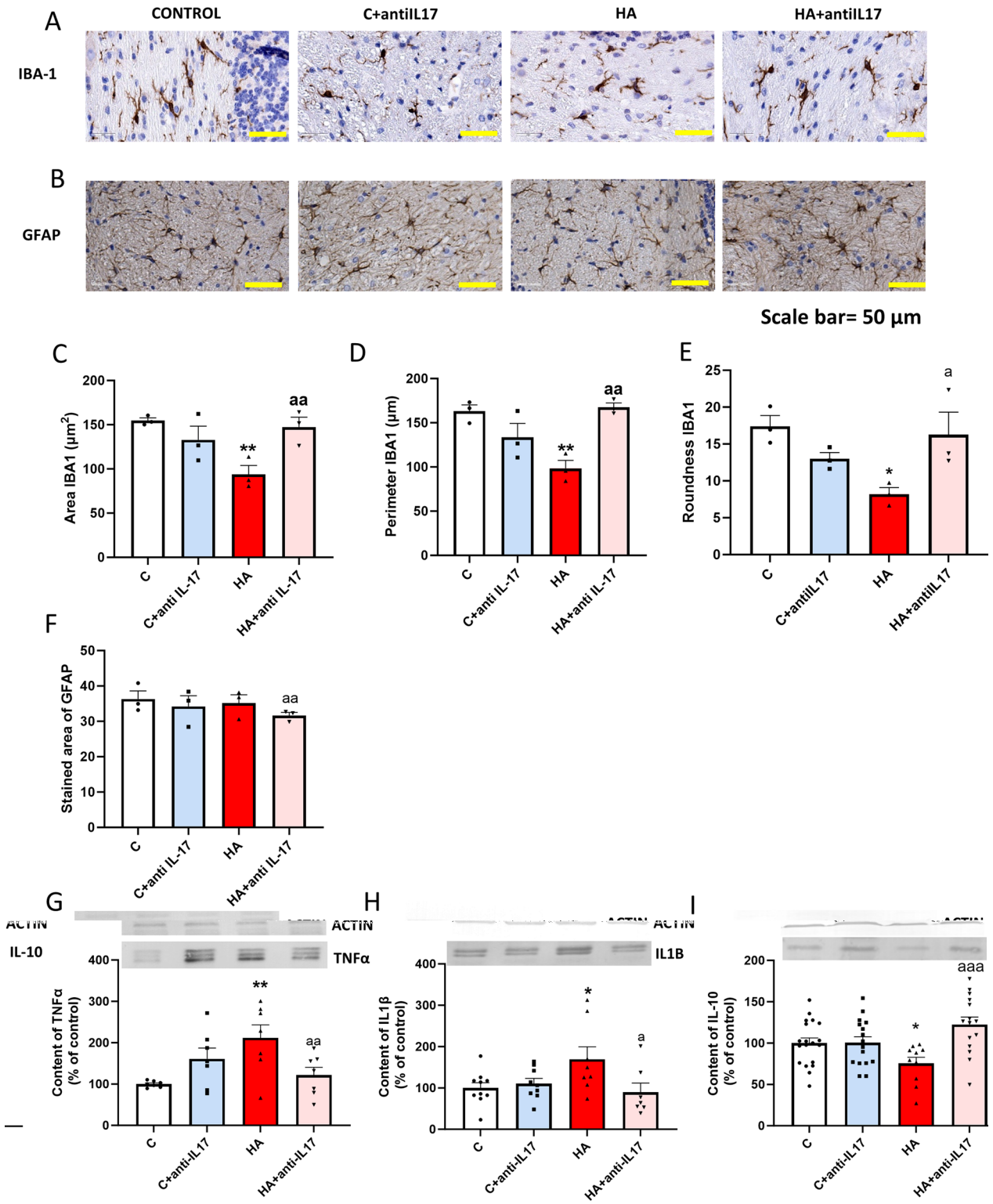


**Fig. 6** (See legend on previous page.)

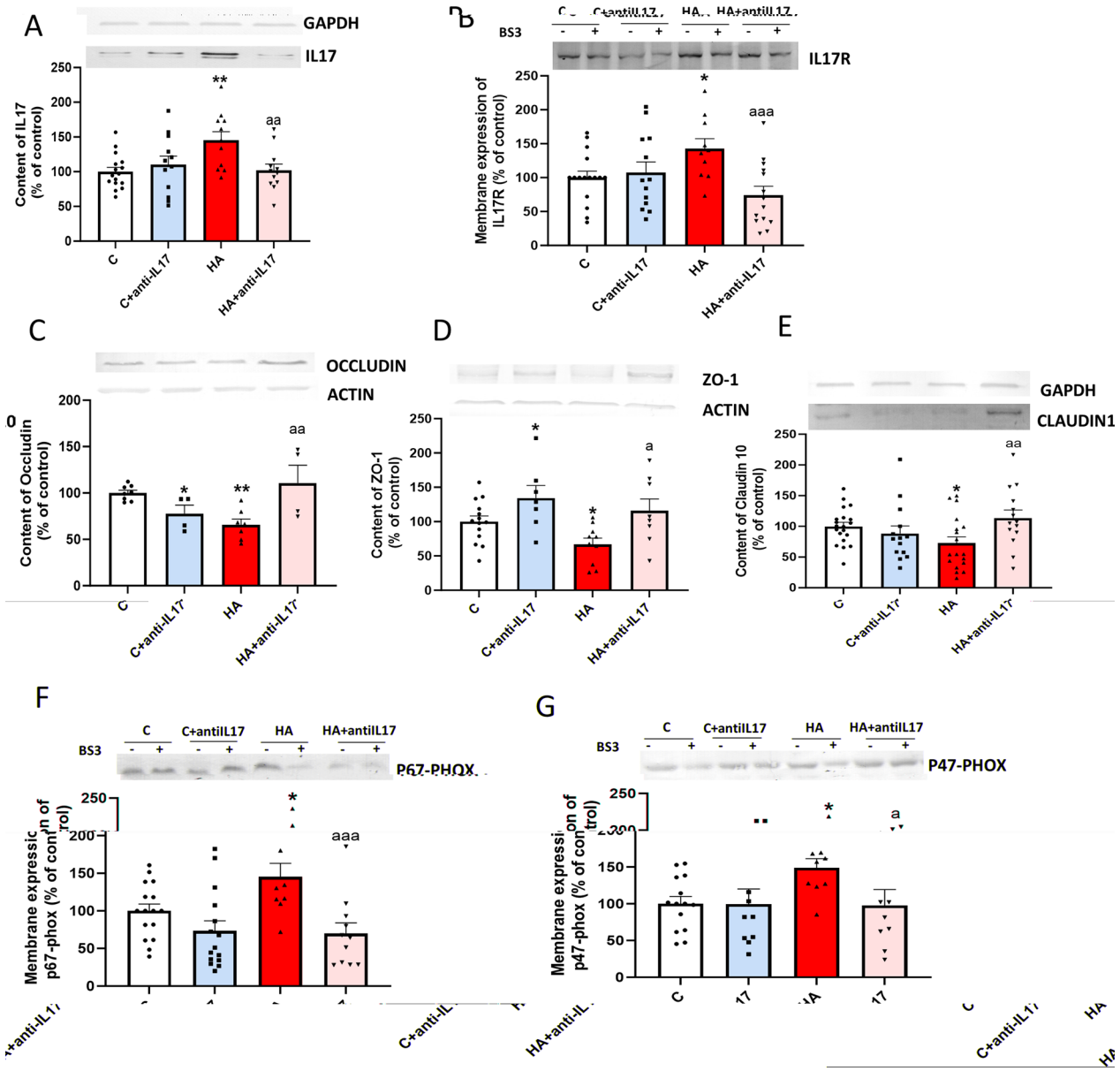


**Fig. 7** Early injection of anti-IL-17 prevents the increase in IL-17 receptor activation and BBB permeabilization and NADPH oxidase activation in cerebellum of hyperammonemic rats at 4 days of hyperammonemia. Protein content of (**A**) IL-17, (**C**) Occludin, (**D**) ZO-1, (**E**) Claudin10, and (**F**) MLCK in cerebellum was analyzed by Western blot. Membrane expression of (**B**) IL17R, (**F**) p67phox and (**G**) p47phox was analyzed using the BS3 cross-linker. Representative images of the blots for each protein are shown. Values are expressed as percentage of controls and are the mean ± SEM of 7 rats/group. One-way ANOVA followed by Fisher's LSD post-hoc test was performed to compare all groups. Values significantly different from controls are indicated by asterisk (*$p < 0.05$, **$p < 0.01$) and values significantly different from HA group are indicated by a (a = $p < 0.05$, aa = $p < 0.01$, aaa = $p < 0.001$)

immune cells drives astrocyte activation. Activated microglia release astrocyte-activating signals which are responsible for astrocyte activation [40, 41]. In the case of hyperammonemic rats the infiltration of CD4 lymphocytes and activation of microglia in cerebellum occurs at 2–3 days of hyperammonemia and it is likely that the production of astrocyte-activating signals by microglia is still not enough at 4 days of hyperammonemia to induce activation of astrocytes, which is clearly observed at longer times of hyperammonemia [9, 10, 42, 43].

Moreover, we also show that blocking peripheral IL-17 with anti-IL-17 during days 2–4 of hyperammonemia prevents CD4 lymphocytes infiltration, microglia

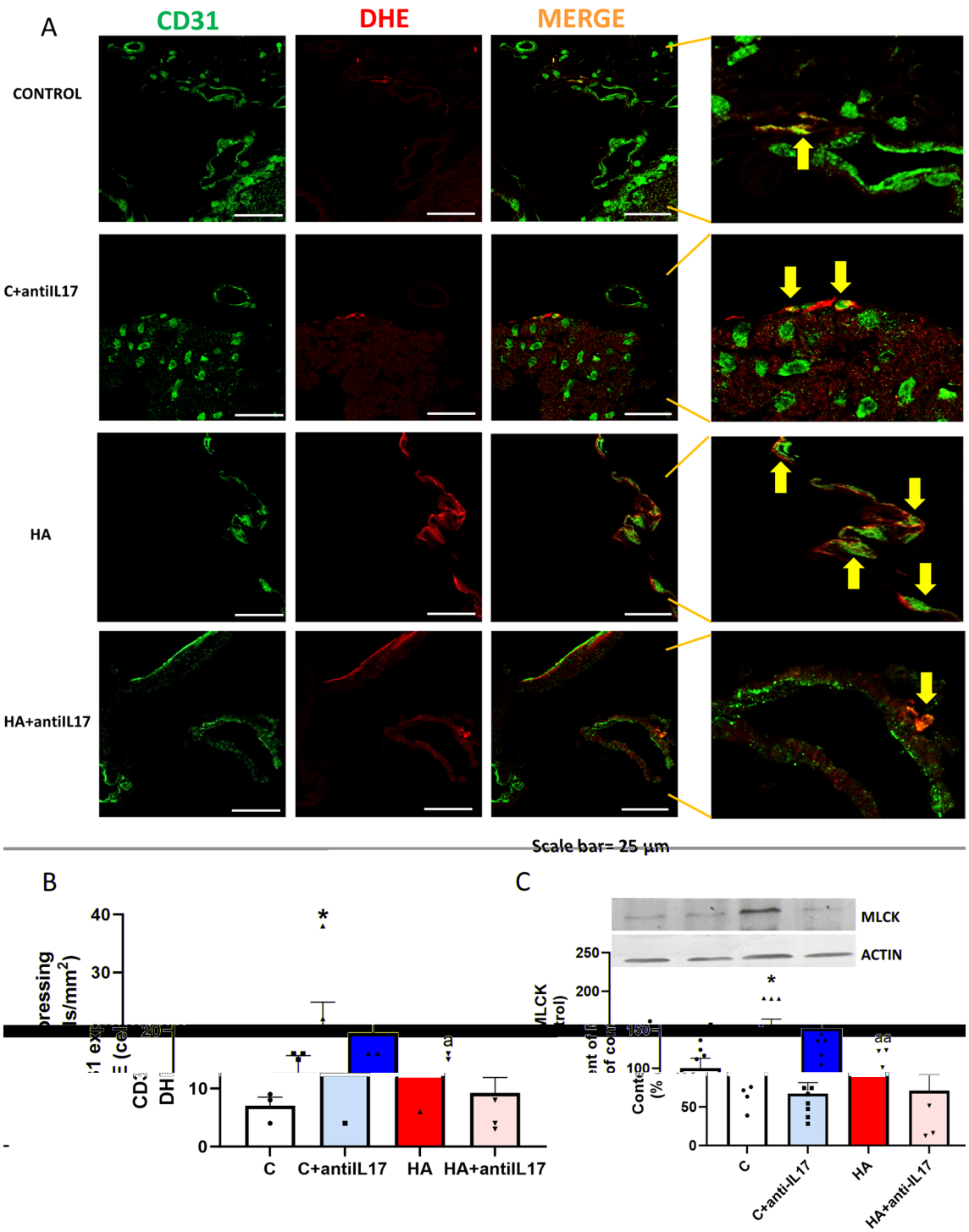


**Fig. 8** Early injection of anti-IL-17 prevents the increase of superoxide production in endothelial cells in the meninges of the cerebellum of hyperammonemic rats. Superoxide was stained with DHE and endothelial cells by immunofluorescence with anti-CD31. Immunofluorescence staining using anti-CD31 (**A**, **B**) shows an increase of CD31 positive endothelial cells that produce superoxide (labeled with DHE) in cerebellar meninges of hyperammonemic rats. The content of MLCK (**C**) in cerebellum was analyzed by Western blot. Representative images of the blots are shown. Values are expressed as percentage of controls. Values are the mean ± SEM of 5 rats/group in **A**, **B** and 7 rats/group in **C**. Values significantly different from control group are indicated by asterisk (*$p < 0.05$, **$p < 0.01$) and values significantly different from HA group are indicated by a (a = $p < 0.05$, aa = $p < 0.01$). Yellow arrows indicate co-localization of the CD31 cells with DHE

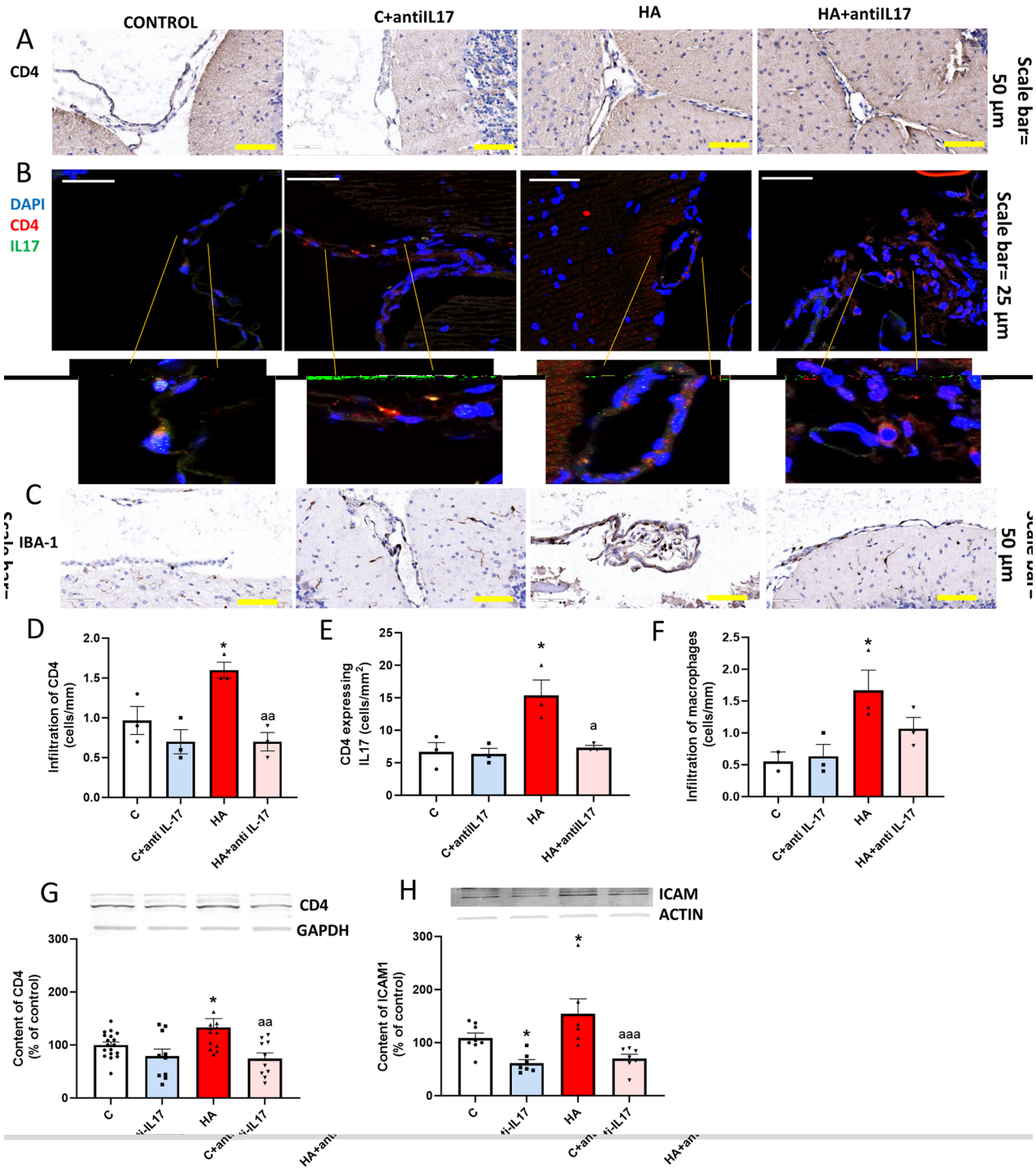


**Fig. 9** Early injection of anti-IL-17 prevents the infiltration of Th17 lymphocytes and monocytes in meninges of cerebellum of hyperammonemic rats. Analysis of CD4 lymphocytes (**A**) and monocyte (**C**) infiltration in the meningeal space of the cerebellum was performed by immunohistochemistry using antibodies against CD4 and Iba1, respectively. Representative images are shown in **A**, **C**. The number of infiltrating $CD4^+$ cells (**D**) and monocytes (**F**) were quantified. Double fluorescence staining using anti-CD4 and IL-17 (**B**, **E**) shows infiltration of Th17 CD4 lymphocytes in the cerebellar meninges of hyperammonemia rats. Protein content of (**G**) CD4 and (**H**) ICAM in cerebellum were analyzed by Western blot. Representative images of the blots of each protein are shown. Values are the mean ± SEM of 3 rats/group in **A**–**F** and 7 rats/group in (G-H). Values significantly different from control group are indicated by asterisk (*$p < 0.05$) and values significantly different from HA group are indicated by a (a = $p < 0.05$, aa = $p < 0.01$, aaa = $p < 0.001$)

activation, and affords sustained prevention of BBB permeabilization and of the enhancement of the TNFα-TNFR1-S1PR2-CCL2-CCR2-BDNF-TrkB pathway, of GABAergic neurotransmission and of motor incoordination, which lasts for at least 5 weeks after anti-IL-17 injection. Hyperammonemia would no longer induce deleterious effects at later phases because the increase in IL-17 in the blood has disappeared.

We have previously shown that systemic inflammation is a crucial intermediary between hyperammonemia, neuroinflammation and neurological impairment [7, 8]. We show here that injection of anti-IL-17 reduces pro-inflammatory cytokines in plasma of hyperammonemic rats, including IL-17 and TNFα. This reduction of peripheral inflammation by anti-IL-17 would also contribute to the beneficial effects in cerebellum.

The induction of BBB permeabilization by increased IL-17 levels in blood has been already reported in other pathological situations, including mice models of multiple sclerosis [31], of Parkinson's disease [44], of perioperative neurocognitive disorders in aging [45] and of sepsis [46].

IL-17 also disrupts the BBB in primary human endothelial cells [28, 47]. The involvement of the IL-17 receptor-NADPH oxidase-superoxide-MLCK-occludin/ZO-1 pathway in the mechanisms leading to BBB permeabilization has been already demonstrated by different groups in other situations [31–34]. We show here that this same mechanism, triggered by blood IL-17, contributes to BBB permeabilization in cerebellum of hyperammonemic rats.

It is noteworthy that a similar induction of BBB permeabilization and induction of neuroinflammation by a transient increase of IL-17 has been reported in patients and animal models of multiple sclerosis (MS). MS patients show increased IL-17 levels in blood and cerebrospinal fluid, which are associated with BBB disruption [25]. Moreover, IL-17 levels tended to decrease with disease duration. Kostic et al. [25] proposed that IL-17 would be more important for MS onset than for disease progression and that this could explain why some MS clinical trials, targeting Th17 cells in the later stage of the disease, failed to provide any clinical benefit [25]. Graber et al. [48] showed that peripheral blood mononuclear cells from patients with early MS produce more IL-17 than those from patients with established MS, further supporting a transient increase of IL-17 in MS similar to that reported here in hyperammonemic rats.

Th17 cells can efficiently cross the BBB, leading to BBB disruption, the activation of other inflammatory cells and neurodegeneration in MS patients [49]. In addition to T lymphocytes, also macrophages may infiltrate the brain in patients with MS, leading to microglia activation [50–52]. A similar infiltration of Th17 CD4 lymphocytes and macrophages has been reported in meninges of cerebellum of patients died with liver disease, associated with hyperammonemia and hepatic encephalopathy [21]. This, together with the increased activation of Th17 and blood levels of IL-17 in cirrhotic patients with minimal hepatic encephalopathy [19] suggests that a similar process to that reported here would trigger motor incoordination and cognitive impairment in these patients. The increase of blood IL-17 levels is transient in hyperammonemic rats, but seems to be sustained in patients with MHE [19]. This suggests that a potential treatment of MHE patients with anti-IL-17 should be chronic.

Permeabilization of the BBB facilitates the infiltration of IL-17 [28–30], which increases in cerebellum at 4 days of hyperammonemia. We have recently shown that IL-17 triggers activation of microglia in cerebellum at 4 weeks of hyperammonemia [42]. A similar IL-17-induced activation of microglia would occur at 4 days of hyperammonemia. Activated microglia produce IL-17 that promotes neuronal damage [53] and TNFα [54, 55] which alters neuronal function [56]. In a similar way, IL-17 driven activation of microglia in cerebellum of hyperammonemia rats increases TNFα production which activates TNFR1 in Purkinje neurons leading to enhanced GABAergic neurotransmission and motor incoordination at 4 weeks of hyperammonemia [42] and also at 4 days of hyperammonemia, as shown here. The mechanisms by which enhanced activation of TNFR1 by TNFα enhances GABAergic neurotransmission and induce motor incoordination have been already described in detail in our previous studies at 4–5 weeks of hyperammonemia [9, 10] and involve enhanced activation of the TNFα-TNFR1-S1PR2-CCL2-CCR2-BDNF-TrkB pathway which

(See figure on next page.)

**Fig. 10** Early injection with anti-IL-17 prevents the alterations in the GABAergic neurotransmission in cerebellum of hyperammonemic rats at 5 weeks of hyperammonemia. Membrane expression of (**A**) $GABA_A\alpha2$, (**B**) $GABA_A\beta3$, (**C**) $GABA_A\gamma2$, (**D**) KCC2, and (**E**) NKCC1 were analyzed using BS3 cross-linker. Representative images of the blots for each protein are shown. Values are expressed as percentage of controls and are the mean ± SEM of 6 rats/group. One-way ANOVA followed by Fisher's LSD post-hoc test was performed to compare all groups. Values significantly different from controls are indicated by asterisk (*$p < 0.05$) and values significantly different from HA group are indicated by a (a = $p < 0.05$, aaa = $p < 0.001$, aaaa = $p < 0.0001$)

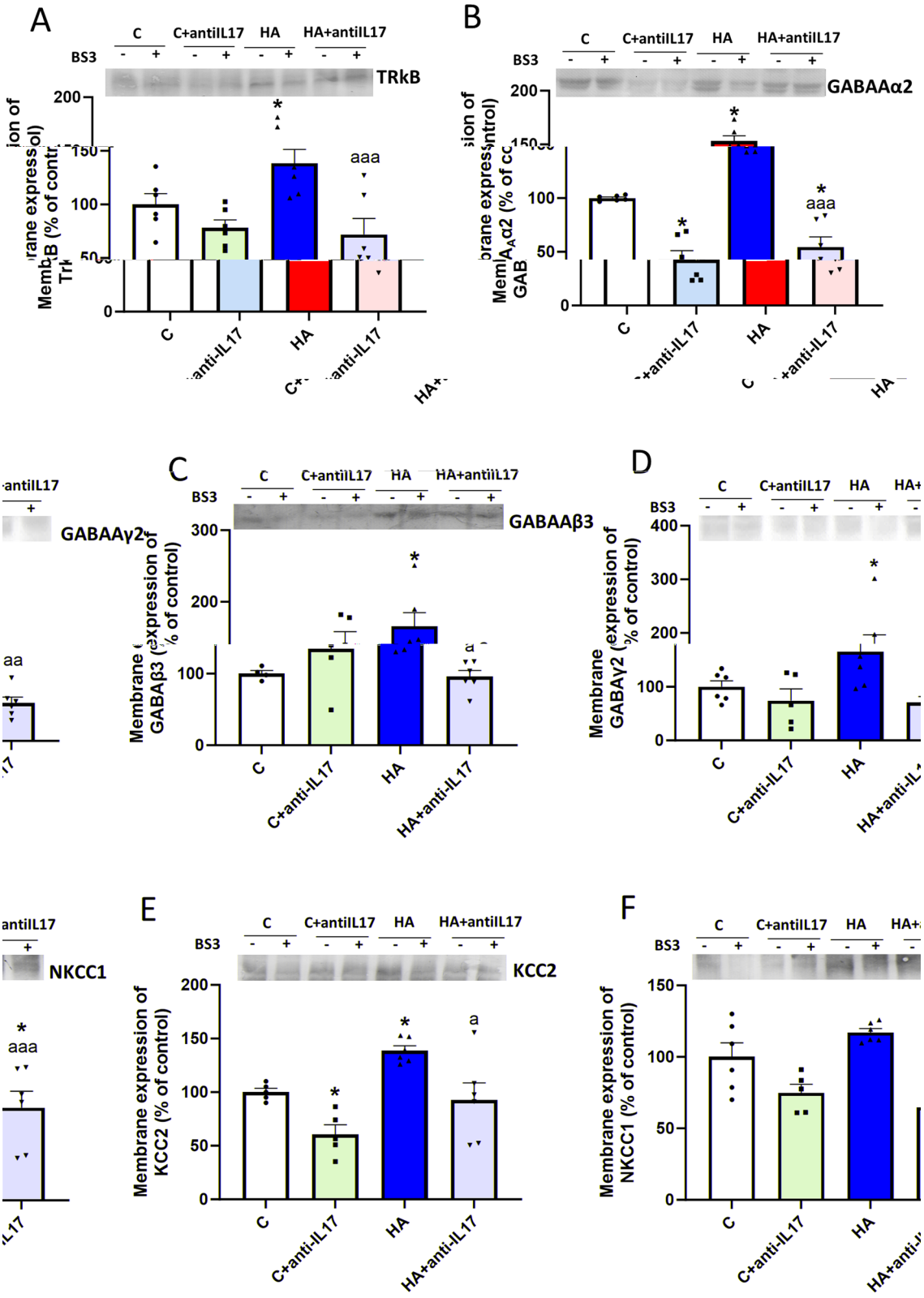


**Fig. 10** (See legend on previous page.)

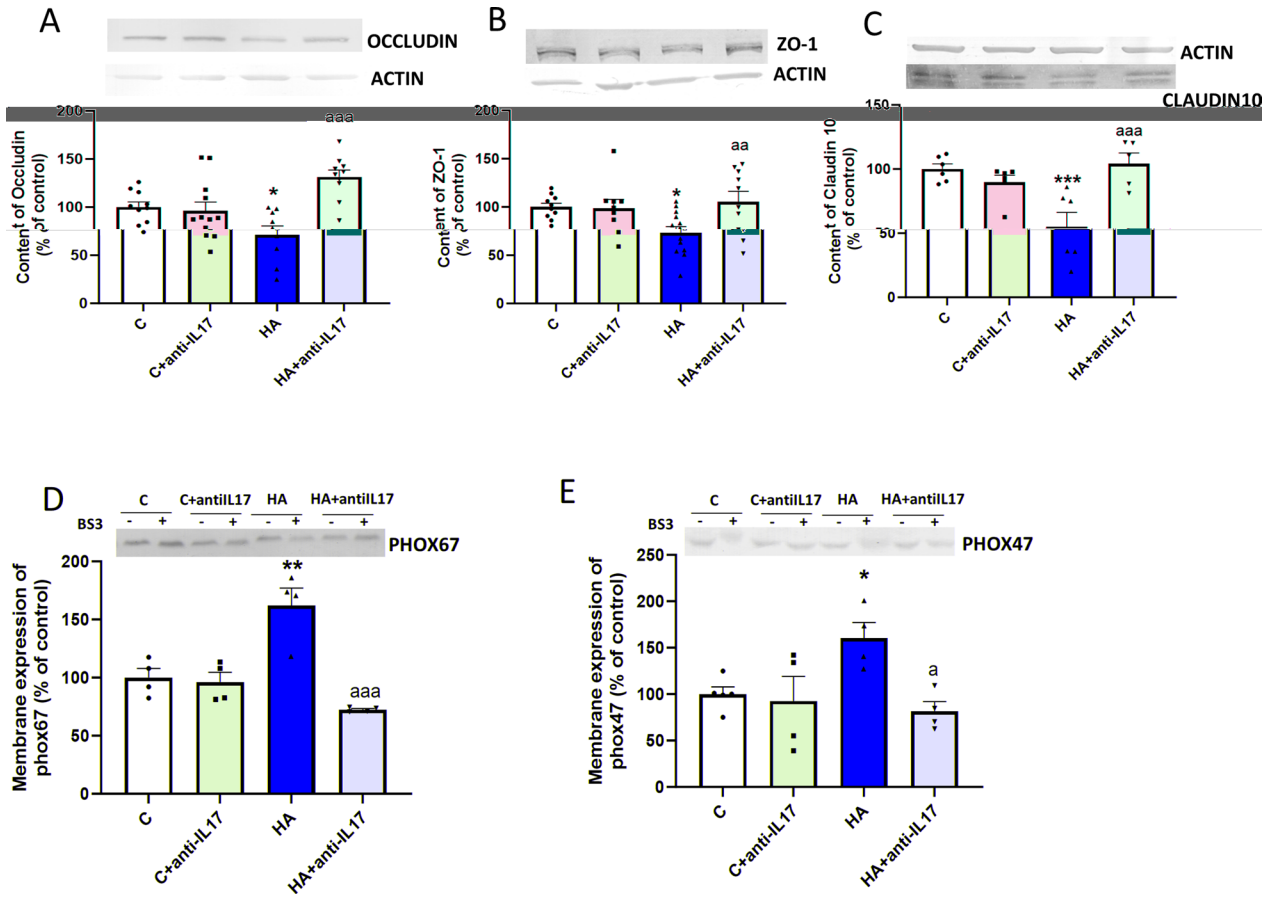


**Fig. 11** Early injection of anti-IL-17 prevents BBB permeabilization and NADPH oxidase activation in cerebellum of hyperammonemic rats at 5 weeks of hyperammonemia. Protein content of (**A**) Occludin, (**B**) ZO-1 and (**C**) Claudin10 in cerebellum was analyzed by Western blot. Membrane expression of (**D**) p67phox and (**E**) p47phox was analyzed using the BS3 cross-linker. Representative images of the blots for each protein are shown. Values are expressed as percentage of controls and are the mean ± SEM of 6 rats/group. One-way ANOVA followed by Fisher's LSD post-hoc test was performed to compare all groups. Values significantly different from controls are indicated by asterisk (*$p < 0.05$, **$p < 0.01$; ***$p < 0.001$) and values significantly different from HA group are indicated by a (a = $p < 0.05$, aa = $p < 0.01$, aaa = $p < 0.001$)

increase membrane expression of $GABA_A$ receptor subunits and of KCC2, leading to enhanced GABAergic neurotransmission [9, 10], which is responsible for motor incoordination in hyperammonemic rats [9, 11, 37, 38, 43, 57]. We show here that this same process is triggered in cerebellum of rats at 4 days of hyperammonemia.

We also show that blocking peripheral blood IL-17 with anti-IL-17 prevents infiltration of lymphocytes and monocytes, permeabilization of the BBB, activation of microglia, induction of neuroinflammation and enhancement of GABAergic neurotransmission as well as induction of motor incoordination by hyperammonemia. These data suggest that early treatment with anti-IL-17 could be a beneficial therapeutic approach in cirrhotic patients at initial stages of minimal hepatic encephalopathy and also in patients with other neurological alterations, including multiple sclerosis.

## Materials and methods

### Rats

Male Wistar rats (120–140 g) were made hyperammonemic by feeding them a diet containing ammonium acetate for 4 days or for 5 weeks as in Felipo et al. [58], and Taoro-Gonzalez et al. [59]. The experiments were approved by the Comite Ético de Experimentación Animal (CEEA) of our center and by the Conselleria de Agricultura of Generalitat Valenciana, and were performed in accordance with the guidelines of the Directive of the European Commission (2010/63/EU) for care and management of experimental animals, and comply with the ARRIVE guidelines for animal research.

### Experimental design

The experimental design is summarized in Fig. 1. For the 3 experiments described below, rats were distributed into four groups: C: control rats injected with phosphate

**Table 1** Effects of hyperamonemia and of treatment with anti-IL-17 on cytokines levels in plasma at 4 days of hyperamonemia

| Cytokine | Hyperammonemic rats (% of control rats) | |
|---|---|---|
| | Basal | Anti-IL-17 |
| TNFα # | 255 ± 53** | 135 ± 27$^{a}$ |
| IL-17 | 149 ± 13* | 96 ± 15$^{a}$ |
| IL-18 | 157 ± 24** | 69 ± 14$^{aaa}$ |
| IL-22 | 133 ± 7** | 72 ± 8$^{aaaa}$ |
| CCL2 | 149 ± 12* | 79 ± 22$^{aa}$ |
| CCL5 | 140 ± 14* | 85 ± 8$^{aa}$ |
| TGFβ | 72 ± 11 | 120 ± 20$^{a}$ |
| IL-4 | 88 ± 7 | 120 ± 13$^{*a}$ |
| IL-10 | 103 ± 11 | 153 ± 19$^{**a}$ |
| IL-6 | 97 ± 10 | 73 ± 7$^{*a}$ |
| CX3CL1 | 102 ± 8 | 107 ± 19 |
| CCL20 | 112 ± 18 | 105 ± 31 |
| IL-15 | 106 ± 14 | 97 ± 24 |

TNF-α was analysed in plasma using an ELISA kit. The remaining cytokines were analysed by Western blot and the data are expressed as percentage of control rats. Values are the mean ± SEM of 7 rats per group. Values significantly different from control rats are indicated by asterisk (*$p < 0.05$, **$p < 0.01$) and from hyperammonemic rats by 'a' (a = $p < 0.05$, aa = $p < 0.01$, aaa = $p < 0.001$, aaaa = $p < 0.0001$)

buffered saline (PBS), C + antiIL-17: control rats injected with antiIL-17, HA: hyperammonemic rats injected with PBS and HA + antiIL-17: injected with antiIL-17.

*Experiment 1*: Ten rats per group. To assess if transient blocking of peripheral IL-17 affords sustained prevention of motor impairment. On day 2 of the ammonium-containing diet, rats were injected in the tail vein either with 4 µg of antiIL-17 in 200 µl or the same volume of PBS as vehicle. Two additional injections were given on days 3 and 4 of the ammonium-containing diet. Analysis of motor coordination and function in the motorater and Catwalk were performed after two weeks of hyperammonemia. Rats were sacrificed after 5 weeks of hyperammonemia. See Fig. 1A. The reason to make an additional injection of anti-IL-17 on day 2 in the in vivo experiment compared to the ex vivo experiments described below was to ensure that we block any possible effect of increased IL-17 in hyperammonemic rats.

*Experiment 2*: Ten rats per group. To analyze underlying mechanisms, rats were intravenously injected in the tail vein after 2 days of hyperammonemia (day 3 of the ammonium-containing diet), either with 4 µg of antiIL-17 in 200 µl or the same volume of PBS as vehicle. A second injection was performed 1 day later and rats were sacrificed after 4 days of hyperammonemia (in the morning of day 5 after beginning the ammonium-containing diet). Some rats were perfused for immunohistochemistry and immunofluorescence analysis (see below). For other rats the cerebellum was removed to analyze the protein content and membrane expression of receptors and transporters as described below. See Fig. 1B.

*Experiment 3*: Five rats per group. To analyze the production of superoxide in endothelial cells in cerebellum, rats were injected with anti-IL-17 as in experiment 2, but, in addition, after 3 days of hyperammonemia rats were also injected intraperitoneally with dihydroethidium (DHE), a probe for superoxide production as described below. After 18 h of DHE injection rats were perfused for immunofluorescence analysis as described below. See Fig. 1C.

#### Blood ammonia

Blood ammonia was measured with a commercial Kit in 20 µL of blood taken from the saphenous vein.

#### Time-course of IL-17 in plasma

Time-course of IL-17 in plasma was analysed by Western blot. Plasma was collected from control and hyperammonemic rats at days 2, 4, 8, 12 and 25 of hyperammonemia in previous studies of the group. Plasma was diluted 1:5 and 75 µg of protein were applied for Western blot as described below.

#### Analysis of peripheral inflammation

Plasma was collected from the saphenous vein of control and hyperammonemic rats at 4 days 2of hyperammonemia. TNFα was measured using an ELISA kit from Invitrogen. All other cytokines in plasma were analyzed by Western blot as described below using antibodies against IL-17 (1:1000), IL-10 (1:1000), IL-18 (1:1000), IL-4 (1:1000), CCL20 (1:1000), TGFβ (1:1000) all from ABCAM, CCL2 (1:2000) from Proteintech, CCL5 (1:500), IL-6 (1:500) and CX3CL1 (1:1000) all from Invitrogen, IL-15 (1:2000) from Bioss, and IL-22 (1:2000) from Bio-Techne. Secondary antibodies (1:4000) against rabbit, mouse, or goat were IgGs conjugated with alkaline phosphatase (Sigma). The images were captured using a Hewlett Packard ScanJet 5300C and band intensities were quantified using AlphaImager 2200 software.

#### Analysis of protein content in cerebellum by Western blot

Control and hyperammonemic rats were sacrificed after 4 days (see above experiments 2 and 3) or 5 weeks (experiment 1) of hyperammonemia. Protein content was analyzed by Western blot in homogenates of the cerebellum. Cerebellum was dissected from 7 rats per group and homogenized in 50 mM TRIS–HCl pH 7.5, 50 mM NaCl, 10 mM EGTA, 5 mM EDTA and protease and phosphatase inhibitors. Protein content was analyzed by Western blot as in Felipo et al. [58], using antibodies

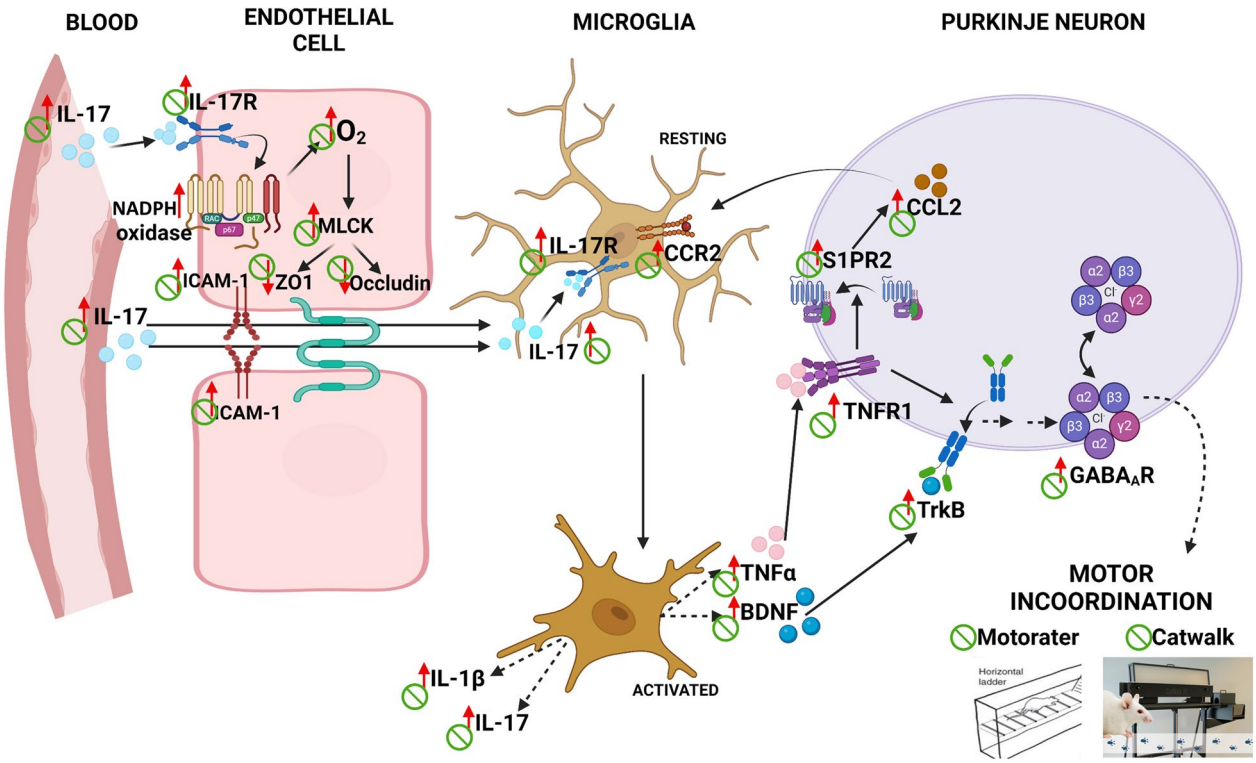


**Fig. 12** Proposed pathway by which a transient increase in blood IL-17 induces neuroinflammation, alterations in GABAergic neurotransmission in cerebellum and motor incoordination in hyperammonemic rats. Hyperammonemia increases blood IL-17 and membrane expression and activation of the IL-17 receptor in endothelial cells, leading to activation of NADPH oxidase, increased superoxide production and MLCK that induce permeabilization of the BBB by reducing occludin and ZO-1 levels. Permeabilization of the BBB facilitates the entry of IL-17, increasing IL-17 in cerebellum, which activates microglia and increase TNFα, which, in turn, activates the TNFα-TNFR1-S1PR2-CCL2-BDNF-TrkB pathway. This enhances membrane expression of $GABA_A$ receptors and of KCC2, leading to increased GABAergic neurotransmission which impairs motor coordination. Early blocking of blood IL-17 with anti-IL-17 prevents all these effects (indicated by *φ* in green). The effects of hyperammonemia are indicated by red arrows (↑). The effects of anti-IL-17 injection are indicated in green *φ*

against IL-17 (1:1000), TrkB (1:500) and IL-10 (1:1000) all from ABCAM, ZO-1 (1:100), CD4 (1:1000) and Occludin (1:300) from NOVUS, TNFα (1:250) and IL1β (1:250) from R&D systems, ICAM (1:1000) and CCL2 (1:2000) and MLCK (1:1000) from Proteintech,, BDNF (1:1000) from Invitrogen, Claudin 10 (1:1000) from Abbomax and actin or GAPDH as a control for protein loading. Secondary antibodies (1:4000) against rabbit, mouse, or goat were IgGs conjugated with alkaline phosphatase (Sigma). The images were captured using a Hewlett Packard ScanJet 5300C and band intensities were quantified using AlphaImager 2200 software.

### Analysis of membrane expression of receptors and transporters

Membrane expression of proteins in cerebellar slices was analyzed by cross-linking with BS3 (Pierce cat# 21580, Rockford, IL, USA) as described in Cabrera-Pastor et al. [60] using antibodies against IL-17R, TrkB, TNFR1 (1:500) from ABCAM, S1PR2 (1:1000) from Proteintek, CCR2 (1:1000) from Novus, GABAγ2 (1:500), GABAβ3 (1:500, ab98968) all from ABCAM, GABAα2 (1:1000) from Bioss Antibodies Inc, P67phox (1:1000) and P47phox (1:1000) from Invitrogen, KCC2 (1:1000) from Millipore and NKCC1 (1:500) from IOWA UNIV t4-s.

Membrane expression of proteins in cerebellar slices was analyzed by cross-linking with BS3 (Pierce cat# 21580, Rockford, IL, USA) as described in Cabrera-Pastor et al. [60]. Slices were added to tubes containing ice-cold Krebs buffer with or without 2 mM bis(sulfosuccinimidyl)suberate (BS3) (Pierce, Rockford, IL, USA) and incubated for 30 min at 4 °C. Cross-linking was terminated by adding 100 mM glycine (10 min, 4 °C). The slices were homogenized by sonication for 20 s. Samples treated with or without BS3 were analysed by Western blot using the above antibodies. BS3 is a cross-linker that reacts with proteins in the membrane surface generating aggregates that do not enter the gel. So that the band in the cytosol is reduced compared to the sample without BS3. The surface expression of receptor subunits

was calculated as the difference between the intensity of the bands without BS3 (total protein) and with BS3 (non-membrane protein) [60].

#### Immunohistochemistry in brain sections

Rats were anaesthetized with sodium pentobarbital and subjected to transcardial perfusion with 0.9% saline followed by 4% paraformaldehyde in 0.1 M phosphate buffer (pH 7.4). The brains were removed and post-fixed in the same fixative for 24 h at 4 °C. Paraffin-embedded sections (5-µm thick) were cut and mounted on coated glass slides, processed with the Envision Flex + Kit (Dako) to block endogenous peroxidase activity for 5 min, and incubated with antibodies against Iba1 (Wako; 1:300), GFAP (SIGMA; 1:400) and CD4 (NOVUS; 1:150) overnight. Then, slides were incubated with Goat anti-mouse or anti-rabbit (biotinylated) secondary antibodies (Vector Laboratories) for 1 h and diaminobenzidine for 10 min. Sections were counterstained with Mayer's hematoxylin (DAKO) for 5 min. Once the slides were dry, they were scanned using an Aperio Versa scanner (Leica Biosystems Nussloch GmbH, Germany). Scanned slides were analyzed using ImageScope64 software, which allows photos of areas of interest to be obtained at different magnifications. In all the immunohistochemistry analyses we include a control without primary antibody where no signal is seen, indicating that the staining reflects true binding of the antibodies.

#### Analysis of astrocytes and microglia activation

Analysis of Iba1 and GFAP staining was performed in the white matter of cerebellar slices using the Image J software as in [9]. Quantification of microglia roundness in the cerebellar white matter was performed with Image pro plus software. Cerebellar slices from three animals per group were used.

#### Analysis of superoxide formation in endothelial cells of cerebellum in vivo

The fluorescent dye DHE was used to analyze superoxide ($O_2^-$) levels in the in the meninges of the cerebellum as in [61]. We performed a parallel experiment in different rats ($n = 5$) as described in Experiment 3 of the experimental design (Fig. 1C). Rats were intravenously injected in the tail vein after 2 days of hyperammonemia, either with 4 µg of antiIL-17 in 200 µL or the same volume of PBS as vehicle. A second injection was performed 1 day later and then the rats were also injected intraperitoneally with 500 µL of DHE (Sigma-Aldrich, 37291). Rats were anesthetized 18 hours after DHE injection using i.p. sodium pentobarbital and were perfused with 4% paraformaldehyde in PBS. Brains were removed and post-fixed in 4% paraformaldehyde for 1 day. Cerebellar sections were cut to do immunofluorescence with antibodies against CD31, a marker of endothelial cells (Bioss, 1:200) overnight and followed the next day by Donkey anti-rabbit Alexa 488 secondary antibody (1:400, Invitrogen). Slices were mounted and evaluated for ethidium fluorescence using Ex λ 358 nm, Em λ greater than 461 nm (ethidium settings). Images were acquired with a Leica TCS SP8 inverted laser scanning confocal microscope using oil objectives: 63X Plan-Apochromat-Lambda Blue 1.4 N.A. Analysis of DHE and CD31 staining was performed in the meninges of the cerebellum using the Image J software. The number of cells positive for CD31 expressing DHE was manually counted using the Cell Counter plugin of ImageJ and the results are expressed as cells/mm$^2$.

#### Analysis of CD4 T-lymphocyte and monocyte infiltration in meninges of cerebellum

Sections were stained with anti-CD4 or anti-Iba1, respectively. Infiltration was analyzed in meningeal spaces. All visible meninges in the slice were photographed. For each case at least 10 fields (40×) were photographed for CD4 and at least eight fields (10×) for Iba1. The number of cells was counted manually. Cell profiles to be counted were defined with discernible nucleus (stained in blue with hematoxylin). Cells for which no nuclei could be distinguished were not counted. Identified cells that show brown staining (DAB) are Iba1- or CD4-positive and were then counted as positive cells. The length of the meninges was measured using ImageJ. The results were expressed as cells/mm. To distinguish infiltrating monocytes from resident microglia, we considered that morphology of resident microglia is very different from that of other brain monocytes-macrophages, allowing us to discriminate one cellular type from the others, as described in [62].

#### Immunofluorescence analysis of the co-localization of CD4 and IL-17 in meningeal spaces

To analyze the infiltration of Th17 CD4 lymphocytes, double immunofluorescence was performed to analyze IL-17 (1:100, ABCAM) co-localization with CD4 for T lymphocyte staining (1:50, NOVUS). Analysis of IL-17 + CD4 staining was performed in the meningeal spaces of the cerebellum using the Image J software which photos were taken using the confocal microscope. The number of CD4 + cells expressing IL-17 in the meningeal spaces of the cerebellum was manually counted using the Cell Counter plugin of ImageJ and the results are expressed as cells/mm$^2$. The analysis for the region was performed on at least 10 40x-fields for each rat.

### Motor function

Motor coordination and locomotor gait parameters were assessed after 3 weeks of anti-IL-17 administration.

### Footprint analysis of locomotor gait in the CatWalk™

This is a video-based automated gait analysis system (Noldus, Wageningen, The Netherlands). Three trials were recorded each day during 2 days as in [63]. Data for regularity index and initial dual stance were analyzed using the CatWalk analysis software (v 7.1) and are the mean of six runs.

### Motor coordination in the MotoRater

A kinematic analysis of motor coordination was conducted using the MotoRater (TSE Systems, Germany) as in [9]. Each day for 2 days, three uninterrupted runs were recorded for each rat. The runs were analysed by counting and classifying the steps as correct or wrong paw placements. The results are expressed as a percentage of total steps and are the mean of six runs.

### Statistical analysis

Results are expressed as mean ± standard error. All statistical analyses were performed using the software program GraphPad Prism v.9.0. Normality was assessed using the D'Agostino and Pearson Omnibus test and the ShapiroWilk normality tests. Differences in variances of normally distributed data were assessed using Bartlett's test. Data with the same variance across groups were analyzed by a parametric one-way analysis of variance (ANOVA) followed by Fisher's LSD multiple comparisons test or two-way ANOVA when appropriate. A confidence level of 95% was accepted as significant. The number of rats used for each parameter and the statistical procedure used in each case is indicated in the corresponding Figure legend.

#### Abbreviations

BBB Blood–brain barrier
CEEA Comite Ético de Experimentación Animal
DHE Dihydroethidium
MHE Minimal hepatic encephalopathy

#### Acknowledgements

Figure 12 has been created with BioRender.com.

#### Author contributions

Conceptualization, V.F. and Y.M.A.; Methodology, Y.M.A; formal analysis, Y.M.A; investigation, Y.M.A, C.M and M.L.; resources, V.F.; data curation, Y.M.A.; writing—original draft preparation, V.F. and Y.M.A.; writing—review and editing, V.F. and Y.M.A.; supervision, M.L. and V.F.; project administration, V.F.; funding acquisition, V.F. and C.M. All authors have read and agreed to the published version of the manuscript.

#### Funding

This manuscript was supported in part by Ministerio de Ciencia e Innovacion Spain (PID2020-113388RB-I00; AEI/https://doi.org/10.13039/501100011033); Conselleria Educacion Generalitat Valenciana (CIPROM 2021/082); European Regional Development Funds / ERDF (PID2020-113388RB-I00 and CIPROM 2021/082). Part of the equipment employed in this work has been funded by Generalitat Valenciana and co-financed with ERDF funds (OP ERDF of Comunitat Valenciana 2014–2020). Instituto de Salud Carlos III (PI23/00062), co-funded ERDF funds. YMAas a Margarita Salas contract at the University of Valencia (MS21-120).

#### Availability of data and materials

No datasets were generated or analysed during the current study.

## Declarations

#### Ethics approval and consent to participate

The experiments were approved by the Comite de Experimentación y Bienestar Animal (CEBA) of Príncipe Felipe Research Center and by the Conselleria de Agricultura of Generalitat Valenciana and were performed in accordance with guidelines of the Directive of the European Commission (2010/63/EU) for care and management of experimental animals.

#### Consent for publication

Not applicable.

#### Competing interests

The authors declare no competing interests.

#### Author details

[1]Laboratory of Neurobiology, Centro de Investigación Príncipe Felipe, Eduardo Primo-Yufera 3, 46012 Valencia, Spain. [2]Departamento de Patología, Facultad de Medicina, Universidad Valencia, Valencia, Spain. [3]INCLIVA Instituto de Investigación Sanitaria, Valencia, Spain.

Received: 12 June 2024 Accepted: 21 November 2024
Published online: 30 November 2024

#### References

1. Shawcross DL, Davies NA, Williams R, Jalan R. Systemic inflammatory response exacerbates the neuropsychological effects of induced hyperammonemia in cirrhosis. J Hepatol. 2004;40(2):247–54. https://doi.org/10.1016/j.jhep.2003.10.016.
2. Blei AT. Infection, inflammation and hepatic encephalopathy, synergism redefined. J Hepatol. 2004;40(2):327–30. https://doi.org/10.1016/j.jhep.2003.12.007.
3. Felipo V, Urios A, Montesinos E, Molina I, Garcia-Torres ML, Civera M, Olmo JA, Ortega J, Martinez-Valls J, Serra MA, Cassinello N, Wassel A, Jordá E, Montoliu C. Contribution of hyperammonemia and inflammatory factors to cognitive impairment in minimal hepatic encephalopathy. Metab Brain Dis. 2012;27(1):51–8. https://doi.org/10.1007/s11011-011-9269-3.
4. Aldridge DR, Tranah EJ, Shawcross DL. Pathogenesis of hepatic encephalopathy: role of ammonia and systemic inflammation. J Clin Exp Hepatol. 2015;5(Suppl 1):S7–20. https://doi.org/10.1016/j.jceh.2014.06.004.
5. Azhari H, Swain MG. Role of peripheral inflammation in hepatic encephalopathy. J Clin Exp Hepatol. 2018;8(3):281–5. https://doi.org/10.1016/j.jceh.2018.06.008.
6. Häussinger D, Dhiman RK, Felipo V, Görg B, Jalan R, Kircheis G, Merli M, Montagnese S, Romero-Gomez M, Schnitzler A, Taylor-Robinson SD, Vilstrup H. Hepatic encephalopathy. Nat Rev Dis Primers. 2022;8(1):43. https://doi.org/10.1038/s41572-022-00366-6.
7. Balzano T, Dadsetan S, Forteza J, Cabrera-Pastor A, Taoro-Gonzalez L, Malaguarnera M, Gil-Perotin S, Cubas-Nuñez L, Casanova B, Castro-Quintas A, Ponce-Mora A, Arenas YM, Leone P, Erceg S, Llansola M, Felipo V. Chronic hyperammonemia induces peripheral inflammation that leads to cognitive impairment in rats: reversed by anti-TNF-α treatment. J Hepatol. 2020;73(3):582–92. https://doi.org/10.1016/j.jhep.2019.01.008.
8. Cabrera-Pastor A, Llansola M, Montoliu C, Malaguarnera M, Balzano T, Taoro-Gonzalez L, García-García R, Mangas-Losada A, Izquierdo-Altarejos P, Arenas YM, Leone P, Felipo V. Peripheral inflammation induces neuroinflammation that alters neurotransmission and cognitive and motor function in hepatic encephalopathy: underlying mechanisms and therapeutic

implications. Acta Physiol (Oxf). 2019;226(2): e13270. https://doi.org/10.1111/apha.13270.
9. Arenas YM, Balzano T, Ivaylova G, Llansola M, Felipo V. The S1PR2-CCL2-BDNF-TrkB pathway mediates neuroinflammation and motor incoordination in hyperammonaemia. Neuropathol Appl Neurobiol. 2022;48(4): e12799. https://doi.org/10.1111/nan.12799.
10. Arenas YM, Martínez-García M, Llansola M, Felipo V. Enhanced BDNF and TrkB activation enhance GABA neurotransmission in cerebellum in hyperammonemia. Int J Mol Sci. 2022;23(19):11770. https://doi.org/10.3390/ijms231911770.
11. Llansola M, Arenas YM, Sancho-Alonso M, Mincheva G, Palomares-Rodriguez A, Doverskog M, Izquierdo-Altarejos P, Felipo V. Neuroinflammation alters GABAergic neurotransmission in hyperammonemia and hepatic encephalopathy, leading to motor incoordination. Mechanisms and therapeutic implications. Front Pharmacol. 2024;15:1358323. https://doi.org/10.3389/fphar.2024.1358323.
12. Williams GP, Schonhoff AM, Sette A, Lindestam Arlehamn CS. Central and peripheral inflammation: connecting the immune responses of Parkinson's disease. J Parkinsons Dis. 2022;12(s1):S129–36. https://doi.org/10.3233/JPD-223241.
13. Cossu D, Hatano T, Hattori N. The role of immune dysfunction in Parkinson's disease development. Int J Mol Sci. 2023;24(23):16766. https://doi.org/10.3390/ijms242316766.
14. Takeda S, Sato N, Morishita R. Systemic inflammation, blood-brain barrier vulnerability and cognitive/non-cognitive symptoms in Alzheimer disease: relevance to pathogenesis and therapy. Front Aging Neurosci. 2014;6:171. https://doi.org/10.3389/fnagi.2014.00171.
15. Sun Y, Koyama Y, Shimada S. Inflammation from peripheral organs to the brain: how does systemic inflammation cause neuroinflammation? Front Aging Neurosci. 2022;14: 903455. https://doi.org/10.3389/fnagi.2022.903455.
16. Liu X, Nemeth DP, Tarr AJ, Belevych N, Syed ZW, Wang Y, Ismail AS, Reed NS, Sheridan JF, Yajnik AR, Disabato DJ, Zhu L, Quan N. Euflammation attenuates peripheral inflammation-induced neuroinflammation and mitigates immune-to-brain signaling. Brain Behav Immun. 2016;54:140–8. https://doi.org/10.1016/j.bbi.2016.01.018.
17. Tieck MP, Vasilenko N, Ruschil C, Kowarik MC. Peripheral memory B cells in multiple sclerosis vs. double negative B cells in neuromyelitis optica spectrum disorder: disease driving B cell subsets during CNS inflammation. Front Cell Neurosci. 2024;18:1337339. https://doi.org/10.3389/fncel.2024.1337339.
18. Dias-Carvalho A, Sá SI, Carvalho F, Fernandes E, Costa VM. Inflammation as common link to progressive neurological diseases. Arch Toxicol. 2024;98(1):95–119. https://doi.org/10.1007/s00204-023-03628-8.
19. Mangas-Losada A, García-García R, Urios A, Escudero-García D, Tosca J, Giner-Durán R, Serra MA, Montoliu C, Felipo V. Minimal hepatic encephalopathy is associated with expansion and activation of $CD^{4+}CD28^{-}$, Th22 and Tfh and B lymphocytes. Sci Rep. 2017;7(1):6683. https://doi.org/10.1038/s41598-017-05938-1.
20. Mangas-Losada A, García-García R, Leone P, Ballester MP, Cabrera-Pastor A, Urios A, Gallego JJ, Martínez-Pretel JJ, Giménez-Garzó C, Revert F, Escudero-García D, Tosca J, Ríos MP, Montón C, Durbán L, Aparicio L, Montoliu C, Felipo V. Selective improvement by rifaximin of changes in the immunophenotype in patients who improve minimal hepatic encephalopathy. J Transl Med. 2019;17(1):293. https://doi.org/10.1186/s12967-019-2046-5.
21. Balzano T, Forteza J, Molina P, Giner J, Monzó A, Sancho-Jiménez J, Urios A, Montoliu C, Felipo V. The cerebellum of patients with steatohepatitis shows lymphocyte infiltration, microglial activation and loss of purkinje and granular neurons. Sci Rep. 2018;8(1):3004. https://doi.org/10.1038/s41598-018-21399-6.
22. Leone P, Arenas YM, Balzano T, Mincheva G, Martinez-Garcia M, Montoliu C, Llansola M, Felipo V. Patients who died with steatohepatitis or liver cirrhosis show neuroinflammation and neuronal loss in hippocampus. Eur J Neurol. 2023;30(10):3032–46. https://doi.org/10.1111/ene.15935.
23. Kerfoot SM, D'Mello C, Nguyen H, Ajuebor MN, Kubes P, Le T, Swain MG. TNF-alpha-secreting monocytes are recruited into the brain of cholestatic mice. Hepatology (Baltimore, MD). 2006;43(1):154–62. https://doi.org/10.1002/hep.21003.
24. D'Mello C, Le T, Swain MG. Cerebral microglia recruit monocytes into the brain in response to tumor necrosis factoralpha signaling during peripheral organ inflammation. J Neurosci. 2009;29(7):2089–102. https://doi.org/10.1523/JNEUROSCI.3567-08.2009.
25. Kostic M, Dzopalic T, Zivanovic S, Zivkovic N, Cvetanovic A, Stojanovic I, Vojinovic S, Marjanovic G, Savic V, Colic M. IL-17 and glutamate excitotoxicity in the pathogenesis of multiple sclerosis. Scand J Immunol. 2014;79(3):181–6. https://doi.org/10.1111/sji.12147.
26. Luchtman DW, Ellwardt E, Larochelle C, Zipp F. IL-17 and related cytokines involved in the pathology and immunotherapy of multiple sclerosis: current and future developments. Cytokine Growth Factor Rev. 2014;25(4):403–13. https://doi.org/10.1016/j.cytogfr.2014.07.013.
27. Lu Y, Zhang P, Xu F, Zheng Y, Zhao H. Advances in the study of IL-17 in neurological diseases and mental disorders. Front Neurol. 2023;14:1284304. https://doi.org/10.3389/fneur.2023.1284304.
28. Kebir H, Kreymborg K, Ifergan I, Dodelet-Devillers A, Cayrol R, Bernard M, Giuliani F, Arbour N, Becher B, Prat A. Human TH17 lymphocytes promote blood–brain barrier disruption and central nervous system inflammation. Nat Med. 2007;13(10):1173–5. https://doi.org/10.1038/nm1651.
29. Voirin AC, Perek N, Roche F. Inflammatory stress induced by a combination of cytokines (IL-6, IL-17, TNF-α) leads to a loss of integrity on bEnd.3 endothelial cells in vitro BBB model. Brain Res. 2020;1730:146647. https://doi.org/10.1016/j.brainres.2020.146647.
30. Chen H, Tang X, Li J, Hu B, Yang W, Zhan M, Ma T, Xu S. IL-17 crosses the blood–brain barrier to trigger neuroinflammation: a novel mechanism in nitroglycerin-induced chronic migraine. J Headache Pain. 2022;23(1):1. https://doi.org/10.1186/s10194-021-01374-9.
31. Huppert J, Closhen D, Croxford A, White R, Kulig P, Pietrowski E, Bechmann I, Becher B, Luhmann HJ, Waisman A, Kuhlmann CR. Cellular mechanisms of IL-17-induced blood-brain barrier disruption. FASEB J. 2010;24(4):1023–34. https://doi.org/10.1096/fj.09-141978.
32. Xie Y, Luo Z, Peng W, Liu Y, Yuan F, Xu J, Sun Y, Lu H, Wu T, Jiang L, Hu J. Inhibition of UTX/KDM6A improves recovery of spinal cord injury by attenuating BSCB permeability and macrophage infiltration through the MLCK/p-MLC pathway. J Neuroinflammation. 2023;20(1):259. https://doi.org/10.1186/s12974-023-02936-1.
33. Li C, Zhang Y, Liu R, Mai Y. Anagliptin protected against hypoxia/reperfusion-induced brain vascular endothelial permeability by increasing ZO-1. ACS Omega. 2021;6(11):7771–7. https://doi.org/10.1021/acsomega.1c00242.
34. Zhai L, Liu M, Wang T, Zhang H, Li S, Guo Y. Picroside II protects the blood-brain barrier by inhibiting the oxidative signaling pathway in cerebral ischemia-reperfusion injury. PLoS ONE. 2017;12(4): e0174414. https://doi.org/10.1371/journal.pone.0174414.
35. Rodrigo R, Cauli O, Gomez-Pinedo U, Agusti A, Hernandez-Rabaza V, Garcia-Verdugo JM, Felipo V. Hyperammonemia induces neuroinflammation that contributes to cognitive impairment in rats with hepatic encephalopathy. Gastroenterology. 2010;139(2):675–84. https://doi.org/10.1053/j.gastro.2010.03.040.
36. Balzano T, Arenas YM, Dadsetan S, Forteza J, Gil-Perotin S, Cubas-Nuñez L, Casanova B, Gracià F, Varela-Andrés N, Montoliu C, Llansola M, Felipo V. Sustained hyperammonemia induces TNF-a IN Purkinje neurons by activating the TNFR1-NF-κB pathway. J Neuroinflammation. 2020;17(1):70. https://doi.org/10.1186/s12974-020-01746-z.
37. Cauli O, Rodrigo R, Piedrafita B, Llansola M, Mansouri MT, Felipo V. Neuroinflammation contributes to hypokinesia in rats with hepatic encephalopathy: ibuprofen restores its motor activity. J Neurosci Res. 2009;87(6):1369–74. https://doi.org/10.1002/jnr.21947.
38. Cabrera-Pastor A, Balzano T, Hernández-Rabaza V, Malaguarnera M, Llansola M, Felipo V. Increasing extracellular cGMP in cerebellum in vivo reduces neuroinflammation, GABAergic tone and motor in-coordination in hyperammonemic rats. Brain Behav Immun. 2018;69:386–98. https://doi.org/10.1016/j.bbi.2017.12.013.
39. Hernández-Rabaza V, Cabrera-Pastor A, Taoro-González L, Malaguarnera M, Agustí A, Llansola M, Felipo V. Hyperammonemia induces glial activation, neuroinflammation and alters neurotransmitter receptors in hippocampus, impairing spatial learning: reversal by sulforaphane. J Neuroinflammation. 2016;13:41. https://doi.org/10.1186/s12974-016-0505-y.
40. Liddelow SA, Guttenplan KA, Clarke LE, Bennett FC, Bohlen CJ, Schirmer L, Bennett ML, Münch AE, Chung WS, Peterson TC, Wilton DK, Frouin A, Napier BA, Panicker N, Kumar M, Buckwalter MS, Rowitch DH, Dawson VL, Dawson TM, Stevens B, Barres BA. Neurotoxic reactive astrocytes are

induced by activated microglia. Nature. 2017;541(7638):481–7. https://doi.org/10.1038/nature21029.
41. Liddelow SA, Barres BA. Reactive astrocytes: production, function, and therapeutic potential. Immunity. 2017;46(6):957–67. https://doi.org/10.1016/j.immuni.2017.06.006.
42. Arenas YM, López-Gramaje A, Montoliu C, Llansola M, Felipo V. Increased levels and activation of the IL-17 receptor in microglia contribute to enhanced neuroinflammation in cerebellum of hyperammonemic rats. Biol Res. 2024;57(1):18. https://doi.org/10.1186/s40659-024-00504-2.
43. Hernandez-Rabaza V, Cabrera-Pastor A, Taoro-Gonzalez L, Gonzalez-Usano A, Agusti A, Balzano T, Llansola M, Felipo V. Neuroinflammation increases GABAergic tone and impairs cognitive and motor function in hyperammonemia by increasing GAT-3 membrane expression. Reversal by sulforaphane by promoting M2 polarization of microglia. J Neuroinflamm. 2016;13(1):83. https://doi.org/10.1186/s12974-016-0549-z.
44. Liu Z, Qiu AW, Huang Y, Yang Y, Chen JN, Gu TT, Cao BB, Qiu YH, Peng YP. IL-17A exacerbates neuroinflammation and neurodegeneration by activating microglia in rodent models of Parkinson's disease. Brain Behav Immun. 2019;81:630–45. https://doi.org/10.1016/j.bbi.2019.07.026.
45. Ni P, Dong H, Wang Y, Zhou Q, Xu M, Qian Y, Sun J. IL-17A contributes to perioperative neurocognitive disorders through blood–brain barrier disruption in aged mice. J Neuroinflammation. 2018;15(1):332. https://doi.org/10.1186/s12974-018-1374-3.
46. Ye B, Tao T, Zhao A, Wen L, He X, Liu Y, Fu Q, Mi W, Lou J. Blockade of IL-17A/IL-17R pathway protected mice from sepsis-associated encephalopathy by inhibition of microglia activation. Mediators Inflamm. 2019;2019:8461725. https://doi.org/10.1155/2019/8461725.
47. Rahman MT, Ghosh C, Hossain M, Linfield D, Rezaee F, Janigro D, Marchi N, van Boxel-Dezaire AHH. IFN-γ, IL-17A, or zonulin rapidly increase the permeability of the blood-brain and small intestinal epithelial barriers: relevance for neuro-inflammatory diseases. Biochem Biophys Res Commun. 2018;507(1–4):274–9. https://doi.org/10.1016/j.bbrc.2018.11.021.
48. Graber JJ, Allie SR, Mullen KM, Jones MV, Wang T, Krishnan C, Kaplin AI, Nath A, Kerr DA, Calabresi PA. Interleukin-17 in transverse myelitis and multiple sclerosis. J Neuroimmunol. 2008;196(1–2):124–32. https://doi.org/10.1016/j.jneuroim.2008.02.008.
49. Balasa R, Barcutean L, Balasa A, Motataianu A, Roman-Filip C, Manu D. The action of TH17 cells on blood brain barrier in multiple sclerosis and experimental autoimmune encephalomyelitis. Hum Immunol. 2020;81(5):237–43. https://doi.org/10.1016/j.humimm.2020.02.009.
50. Kaushik DK, Bhattacharya A, Lozinski BM, Wee Yong V. Pericytes as mediators of infiltration of macrophages in multiple sclerosis. J Neuroinflamm. 2021;18(1):301. https://doi.org/10.1186/s12974-021-02358-x.
51. Veroni C, Serafini B, Rosicarelli B, Fagnani C, Aloisi F, Agresti C. Connecting Immune cell infiltration to the multitasking microglia response and TNF receptor 2 induction in the multiple sclerosis brain. Front Cell Neurosci. 2020;14:190. https://doi.org/10.3389/fncel.2020.00190.
52. Vanderlocht J, Hellings N, Hendriks JJ, Stinissen P. The ambivalent nature of T-cell infiltration in the central nervous system of patients with multiple sclerosis. Crit Rev Immunol. 2007;27(1):1–13. https://doi.org/10.1615/critrevimmunol.v27.i1.10.
53. Lv M, Liu Y, Zhang J, Sun L, Liu Z, Zhang S, Wang B, Su D, Su Z. Roles of inflammation response in microglia cell through Toll-like receptors 2/interleukin-23/interleukin-17 pathway in cerebral ischemia/reperfusion injury. Neuroscience. 2011;176:162–72. https://doi.org/10.1016/j.neuroscience.2010.11.066.
54. Lee EJ, Moon PG, Baek MC, Kim HS. Comparison of the effects of matrix metalloproteinase inhibitors on TNF-α release from activated microglia and TNF-α converting enzyme activity. Biomol Therapeut. 2014;22(5):414–9. https://doi.org/10.4062/biomolther.2014.099.
55. Newell EA, Exo JL, Verrier JD, Jackson TC, Gillespie DG, Janesko-Feldman K, Kochanek PM, Jackson EK. 2',3'-cAMP, 3'-AMP, 2'-AMP and adenosine inhibit TNF-α and CXCL10 production from activated primary murine microglia via A2A receptors. Brain Res. 2015;1594:27–35. https://doi.org/10.1016/j.brainres.2014.10.059.
56. Klapal L, Igelhorst BA, Dietzel-Meyer ID. Changes in neuronal excitability by activated microglia: differential Na(+) current upregulation in pyramid-shaped and bipolar neurons by TNF-α and IL-18. Front Neurol. 2016;7:44. https://doi.org/10.3389/fneur.2016.00044.
57. Gonzalez-Usano A, Cauli O, Agusti A, Felipo V. Pregnenolone sulfate restores the glutamate-nitric-oxide-cGMP pathway and extracellular GABA in cerebellum and learning and motor coordination in hyperammonemic rats. ACS Chem Neurosci. 2014;5(2):100–5. https://doi.org/10.1021/cn400168y.
58. Felipo V, Miñana MD, Azorín I, Grisolía S. Induction of rat brain tubulin following ammonium ingestion. J Neurochem. 1988;51(4):1041–5. https://doi.org/10.1111/j.1471-4159.1988.tb03065.x.
59. Taoro-Gonzalez L, Arenas YM, Cabrera-Pastor A, Felipo V. Hyperammonemia alters membrane expression of GluA1 and GluA2 subunits of AMPA receptors in hippocampus by enhancing activation of the IL-1 receptor: underlying mechanisms. J Neuroinflamm. 2018;15(1):36. https://doi.org/10.1186/s12974-018-1082-z.
60. Cabrera-Pastor A, Taoro L, Llansola M, Felipo V. Roles of the NMDA receptor and EAAC1 transporter in the modulation of extracellular glutamate by low and high affinity AMPA receptors in the cerebellum in vivo: differential alteration in chronic hyperammonemia. ACS Chem Neurosci. 2015;6(12):1913–21. https://doi.org/10.1021/acschemneuro.5b00212.
61. Quick KL, Dugan LL. Superoxide stress identifies neurons at risk in a model of ataxia-telangiectasia. Ann Neurol. 2001;49(5):627–35. https://doi.org/10.1002/ana.1005.
62. Lee E, Eo JC, Lee C, Yu JW. Distinct features of brain-resident macrophages: microglia and non-parenchymal brain macrophages. Mol Cells. 2021;44(5):281–91. https://doi.org/10.14348/molcells.2021.0060.
63. Mincheva G, Gimenez-Garzo C, Izquierdo-Altarejos P, Martinez-Garcia M, Doverskog M, Blackburn TP, Hällgren A, Bäckström T, Llansola M, Felipo V. Golexanolone, a $GABA_A$ receptor modulating steroid antagonist, restores motor coordination and cognitive function in hyperammonemic rats by dual effects on peripheral inflammation and neuroinflammation. CNS Neurosci Ther. 2022;28(11):1861–74. https://doi.org/10.1111/cns.13926.

## Publisher's Note